

RESEARCH ARTICLE

Reliance of deep-sea benthic macrofauna on ice-derived organic matter highlighted by multiple trophic markers during spring in Baffin Bay, Canadian Arctic

Gustavo Yunda-Guarin^{1,*}, Thomas A. Brown², Loïc N. Michel³, Blanche Saint-Béat¹, Rémi Amiraux¹, Christian Nozais⁴, and Philippe Archambault¹

Benthic organisms depend primarily on seasonal pulses of organic matter from primary producers. In the Arctic, declines in sea ice due to warming climate could lead to changes in this food supply with as yet unknown effects on benthic trophic dynamics. Benthic consumer diets and food web structure were studied in a seasonally ice-covered region of Baffin Bay during spring 2016 at stations ranging in depth from 199 to 2,111 m. We used a novel combination of highly branched isoprenoid (HBI) lipid biomarkers and stable isotope ratios ($\delta^{13}\text{C}$, $\delta^{15}\text{N}$) to better understand the relationship between the availability of carbon sources in spring on the seafloor and their assimilation and transfer within the benthic food web. Organic carbon from sea ice (sympagic carbon [SC]) was an important food source for benthic consumers. The lipid biomarker analyses revealed a high relative contribution of SC in sediments (mean SC% \pm standard deviation [SD] = 86% \pm 16.0, $n = 17$) and in benthic consumer tissues (mean SC% \pm SD = 78% \pm 19.7, $n = 159$). We also detected an effect of sea-ice concentration on the relative contribution of SC in sediment and in benthic consumers. Cluster analysis separated the study region into three different zones according to the relative proportions of SC assimilated by benthic macrofauna. We observed variation of the benthic food web between zones, with increases in the width of the ecological niche in zones with less sea-ice concentration, indicating greater diversity of carbon sources assimilated by consumers. In zones with greater sea-ice concentration, the higher availability of SC increased the ecological role that primary consumers play in driving a stronger transfer of nutrients to higher trophic levels. Based on our results, SC is an important energy source for Arctic deep-sea benthos in Baffin Bay, such that changes in spring sea-ice phenology could alter benthic food-web structure.

Keywords: Benthic food webs, Trophic markers, Sea-ice algae, Climate change, HBIs, Stable isotopes, Baffin Bay, Arctic Ocean

Introduction

In the Arctic Ocean, the functioning of the food web is linked to the dynamics of sea ice (Kędra et al., 2015). Indeed, the development of marine primary production, based on unicellular microalgae associated with sea ice (i.e., sympagic or ice algae) and with the water column

(i.e., phytoplankton; Frey et al., 2018), is strongly influenced by sea-ice dynamics. During spring, when the snow melts and sea ice becomes more transparent, the growth of sea-ice algae provides the first substantial carbon input to the food web, being consumed by sea-ice fauna, zooplankton, and benthic organisms (Nozais et al., 2001; Tremblay et al., 2006; Link et al., 2011). Depending on latitude and sea-ice conditions in regions with seasonal sea-ice cover, sympagic primary production rates range from 2×10^{-3} to $20 \text{ g C m}^{-2} \text{ year}^{-1}$, representing 1%–26% of total production in these areas (Gosselin et al., 1997; Tamelander et al., 2009; Leu et al., 2011). Up to $6.5 \text{ g C m}^{-2} \text{ year}^{-1}$ of particulate organic matter (OM) originating from this production sinks into the deep ocean (Boetius et al., 2013). As a result, sea ice constitutes a natural regulator of energy transfer through trophic links (North et al., 2014; Calizza et al., 2018) and strengthens pelagic-benthic coupling (Piepenburg, 2005).

¹ ArcticNet, Québec Océan, Takuvik, Université Laval, Québec, Canada

² The Scottish Association for Marine Science, Oban, Scotland, United Kingdom

³ Centre de Bretagne, REM/EEP, Institut Français de Recherche pour l'Exploitation de la Mer (Ifremer), Laboratoire Environnement Profond, Plouzané, France

⁴ Département de biologie, chimie et géographie, Université du Québec à Rimouski, Rimouski, Canada

* Corresponding author:

Email: gustavo-adolfo.guarin.1@ulaval.ca

The response of marine food webs to variations in the organic carbon cycle is one of the fundamental issues in the changing Arctic Ocean due to the sensitivity of food webs to changes in the magnitude and direction of energy flow (Findlay et al., 2015). For a long time, the deep (below 200-m water depth) seafloor ecosystem was considered largely unaffected by the human footprint (Bluhm et al., 2011). Evidence suggests, however, that deep-sea ecosystems can be influenced by climate-driven seasonal and interannual changes taking place in shallower waters (Glover et al., 2010); for example, climate change may affect the availability of carbon resources across different depths in the ocean (Divine et al., 2015). As benthic communities depend primarily on seasonal pulses of OM that reach the seabed, variations in the timing or quantity of this food supply can influence interactions, abundance, and distribution of benthic fauna (Collin et al., 2011; Roy et al., 2014; Vedenin et al., 2018), with consequences for food web functioning that are not yet fully understood (Van Oevelen et al., 2011; Jeffreys et al., 2013; North et al., 2014; Keđra et al., 2015; Griffiths et al., 2017; Mäkelä et al., 2017). Some benthic fauna seem to be able to change diet rapidly and ingest a wide range of food sources (e.g., plant detritus, animal carcasses, bacteria, and fungi; Gage, 2003), which makes identifying the sources of carbon and assessing proportions ingested by consumers difficult (Kelly and Scheibling, 2012). The absence of such information can hinder accurate predictions of the response of benthic consumers to changes in food supply. Although the OM originating from the water column is already known to be an essential food source for benthic fauna at different depths, studies of the transfer of sympagic carbon (SC) to deep benthic consumers are scarce (e.g., Link et al., 2011; Boetius et al., 2013; Jeffreys et al., 2013). Recently, novel approaches that use multiple trophic markers (e.g., fatty acids and stable isotope ratios) have opened new research avenues in the attempt to differentiate with more accuracy the proportions of OM sources in the environment (Leu et al., 2020) and in consumers (Budge et al., 2008; Wang et al., 2015).

HBI is a lipid biomarker found frequently in marine and lacustrine sediments (Volkman et al., 1994; Belt et al., 2007; Brown and Belt, 2016). Among HBIs, a monounsaturated HBI termed IP₂₅ (Belt et al., 2007) and its homolog, a di-unsaturated HBI II (diene, often referred to as IPSO₂₅ in the Antarctic), have been used as proxies of SC in the environment (Xu et al., 2006; Brown et al., 2016), notably in Arctic benthic organisms (Brown et al., 2012; Brown and Belt, 2012; Brown et al., 2013). In contrast with sea-ice proxies, a further tri-unsaturated HBI (often referred to as HBI III or triene) has been proposed as a promising proxy for pelagic OM (phytoplankton) in the region of open waters near the marginal ice zone (MIZ) in polar regions (Belt, 2018; Belt et al., 2019). Based on the relative abundances of pelagic (III) and sympagic (IP₂₅, II) lipid biomarkers, quantitative estimates of the relative proportions of SC transfer through different trophic levels have been calculated (Brown et al., 2017a, 2017b, 2018; Brown and Belt, 2017), revealing the importance of each OM source in the diet of different organisms across the Arctic

food web. For example, the HBI-fingerprint, or “H-Print,” is an index that has been used to estimate the relative contribution of both sympagic and pelagic carbon sources (Brown et al., 2014).

Besides lipid markers, carbon and nitrogen stable isotope ratios are effective tools for the study of the structure and dynamics of food webs, as they provide time- and space-integrated insights into trophic relationships (Layman and Allgeier, 2012). Because of an often consistent gradual ¹⁵N-enrichment of 2.3‰ per trophic step in aquatic environments (McCutchan et al., 2003), nitrogen isotope ratios (δ¹⁵N) are used to estimate the trophic level of consumers. On the other hand, with a 0‰–2‰ of ¹³C-enrichment per trophic step, carbon isotope ratios (δ¹³C) are typically used to establish the dependence of benthic macrofauna on different food sources (Renaud et al., 2015). Original multidimensional metrics were made to represent the total extent of the ecological diversity using stable isotopes only (Layman et al., 2007). In the present study, HBI lipid biomarkers were coupled quantitatively with stable isotopes to generate community-wide niche proxies combining insights from both methods. To our knowledge, this approach is unique in the literature. Metrics derived from this kind of analysis can give additional clues to understand the changes in food web structures in areas exposed to marked seasonal changes in sea-ice phenology and primary productivity.

To assess the relative importance of SC as a food source to deep benthic communities, we conducted a field investigation of macrobenthos in areas near the MIZ. Baffin Bay provides an ideal natural laboratory to investigate the effects of sympagic production availability on benthic food web structure and functioning. In Baffin Bay, sea ice starts forming in late autumn and reaches maximum extent around March, with ice melt beginning as early as April (Stern and Heide-Jørgensen, 2003). Excluding the ice-free months between August and September, Baffin Bay is always moderately covered by sea ice (Tang et al., 2004). Ocean currents and the atmospheric temperature influence the extent and formation of sea ice in the south of Baffin Bay (Stern and Heide-Jørgensen, 2003). On its eastern side, the West Greenland Current moves warm Atlantic waters northward along the western coast of Greenland (Bi et al., 2019). On its western side, the Baffin Current carries cold Arctic waters and sea ice southward along the east coast of Baffin Island, toward the Labrador Sea (**Figure 1A**; Bi et al., 2019). This distinct longitudinal gradient in sea-ice concentration (SIC) thus presents an important feature against which to test the effects of sea-ice decline on the availability of different carbon sources for deep benthic consumers and how further ice loss could affect deep communities around the Arctic. Moreover, this region is undergoing one of the most significant declines in sea ice in the Canadian Arctic Ocean, as the sea-ice extent was reduced by 102,000 km² between 1968 and 2018 (Environment and Climate Change Canada, 2019). As a result of changes in atmospheric and oceanic temperatures, with an earlier onset of sea-ice melt in spring (4.6 days per decade; Arctic Monitoring and Assessment Programme [AMAP], 2018), a continuous reduction

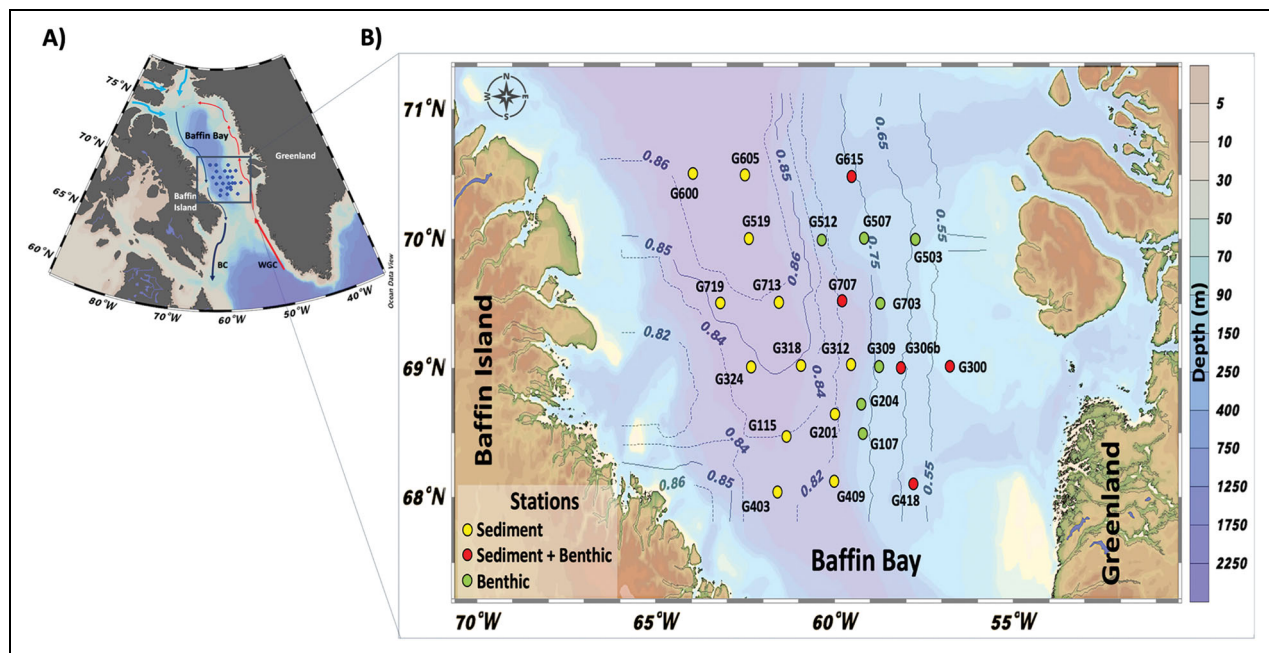


Figure 1. Location of the sampling stations with bathymetry gradients. Red arrows show the northward-flowing West Greenland Current, and blue arrows show the southward-flowing Baffin Current (Map A). Colored points show sampling stations (June 11 to July 10, 2016) for sediment only (yellow), both sediment and benthic macrofauna (red), and benthic macrofauna only (green; Map B). The average sea-ice concentration, ranging from 0% to 100% (expressed here between 0 and 1; gray lines), in the spring (April 1 to June 30 between 1998 and 2017) were derived from the National Snow and Ice Data Center (<https://nsidc.org/data/nsidc-0051>). DOI: <https://doi.org/10.1525/elementa.2020.047.f1>

in sea-ice thickness and extent (10%–15% in spring by 2080) is predicted in Baffin Bay. Using an innovative coupling of sea-ice algae lipid biomarker and stable isotope analyses, the following hypotheses were tested: (1) Sea-ice cover is the primary environmental driver of contribution and geographic distribution of SC on the seabed, (2) SC is the most important baseline food source supporting benthic consumers during spring in areas close to the MIZ, and (3) deep benthic food web dynamics and structural variability are directly linked with both depth and availability of food sources.

Materials and methods

Study area and sampling collection

This study was conducted on board the Canadian research icebreaker CCGS *Amundsen* in Baffin Bay (Figure 1A). Twenty-four stations near the MIZ were sampled for sediments and macrofauna from June 11 to July 10, 2016, within the framework of the Green Edge project (www.greenedgeproject.info). Station depths ranged from 199 to 2,111 m. Epibenthic fauna were collected at 12 stations (Figure 1B: red and green colored stations) using an Agassiz trawl with an opening of 1.5 m and a net mesh size of 40 mm. Box core (0.125 m²) sampling was undertaken to collect surface sediment samples (upper 1 cm) at 17 stations (Figure 1B: red and yellow-colored stations). For each box core, six sediment subcores were collected for sediment pigment content (with 10-ml truncated syringes of an area of 1.5 cm²), granulometry, organic carbon content, HBIs, and stable isotope analyses (with 60-ml

truncated syringes of an area of 5 cm²). Ice blocks containing fresh sympagic algae were collected at three stations (G115, G318, and G409; Figure 1B). After collection, all samples were frozen immediately at –20°C for further analysis. Sediment porosity was estimated by measuring the mass loss of the wet sediment dried at 60°C; total OM content was determined as the ash-free dry weight after combustion (500°C) and converted to total OM in the sediment. Chlorophyll *a* (Chl *a*) content was determined fluorometrically following the protocol of Riaux-Gobin and Klein (1993). Water samples were collected 10 m above the seafloor using a CTD-Rosette with 12-L Niskin-type bottles to determine the isotopic composition of the suspended particular organic matter (SPOM) close to the bottom. The water was filtered onto precombusted filters (450°C for 5 h) of 21-mm diameter Whatman GF/F glass-fiber filters (nominal pore size of 0.7 μm).

Extraction and quantification of HBI lipid biomarkers

In the laboratory, benthic macrofauna were separated, weighed, and identified to the lowest taxonomic resolution possible. A total of 648 individuals were processed for the extraction and quantification of HBIs. Due to their small size, some individuals had to be pooled by species per station, resulting in 249 samples processed for subsequent HBI measurements (Table S1). Lipid extraction and quantification of surface sediment samples was carried out for 17 stations. Processed samples that did not contain all three types of HBIs were discarded from the analyses, as

a combination of sympagic and pelagic HBIs is required to calculate the “H-Print” biomarker index (Equation 1) and the percentage of SC (Equation 2).

The extraction of HBIs was carried out at Laval University, Québec, Canada, while the HBI analyses were done in the marine ecology and chemistry laboratory at the Scottish Association for Marine Science, Scotland, following established techniques (Belt et al., 2012). Molecular structures of HBI alkenes measured in this study (IP₂₅, diene, and triene) can be found in Figure S1. HBIs were analyzed by gas chromatography-mass spectrometry and quantified by measuring the mass spectral intensities for each HBI in selective ion monitoring mode (Brown et al., 2017a). The data were obtained and analyzed using the Agilent ChemStation software.

SC quantification

To quantify the contribution of sympagic algae as a food source, the “H-Print” biomarker index was calculated combining the analytical intensities of three HBI biomarkers, IP₂₅ (*m/z* 350.3), II (*m/z* 348.3), and III (*m/z* 346.3), into a single index, according to Equation 1 (Brown and Belt, 2017). High values of H-Print (>50%) are associated with pelagic carbon, and lower values (<50%) are associated with SC.

H-Print (%)

$$= \frac{\text{Pelagic HBI (III)}}{\text{Sympagic HBIs (IP}_{25} + \text{II}) + \text{Pelagic HBI (III)}} \times 100. \quad \text{Equation(1)}$$

To estimate the relative proportion of SC in sediments and benthic fauna, we used Equation 2 proposed by Brown et al. (2018). It is based on a previously established calibration that converts the H-Print values into estimates of SC (Brown and Belt, 2017). To calculate the relative proportion of OM derived from sea ice (ice organic matter, iOM), we used Equation 3 whereby the OM percentage in sediments (OM, %) is multiplied by the SC estimation from Equation 2.

$$\text{Sympagic carbon (SC, \%)} = 101.08 - 1.02 \times \text{H-Print (\%)}, \quad \text{Equation(2)}$$

$$\text{Ice organic matter (iOM, \%)} = \text{SC (\%)} \times \text{OM (\%)}. \quad \text{Equation(3)}$$

Carbon and nitrogen stable isotope analyses

Sediments and benthic fauna that had been previously treated (i.e., lipid extraction) for HBI analyses were freeze-dried at -50°C and ground to a fine powder with mortar and pestle. HCl was used to remove carbonates prior to stable carbon isotopic ($\delta^{13}\text{C}$) analysis. Surface sediment and organisms with significant carbonate structures, for example, echinoderms, were soaked in 1 N HCl until bubbling ceased. The stable nitrogen isotopic ($\delta^{15}\text{N}$) composition was determined on nonacidified samples to avoid the alteration of $\delta^{15}\text{N}$ values (Roy et al.,

2015). Stable nitrogen isotope ratios were measured using a continuous-flow isotope ratio mass spectrometer (Thermo Electron Delta Advantage) in the continuous-flow mode (Thermo Electron ConFlo III) with an ECS 4010 Elemental Analyzer/ZeroBlank Autosampler (Costech Analytical Technologies) in the laboratory of oceanography at Laval University, Quebec, Canada. Replicate measurements of international standards (USGS40 and USGS41 from the International Atomic Energy Agency; B2151 from Elemental Microanalysis) established measurement errors of $\leq 0.2\text{‰}$ for $\delta^{13}\text{C}$ and $\delta^{15}\text{N}$. Stable isotope ratios are expressed in delta (δ) units ($\delta^{13}\text{C}$, $\delta^{15}\text{N}$) as the per mil (‰) difference with respect to standards: $\delta X(\text{‰}) = [(R_{\text{sample}} - R_{\text{standard}})/R_{\text{standard}}] \times 10^3$, where X is ^{13}C or ^{15}N of the sample and R is the corresponding ratio $^{13}\text{C}/^{12}\text{C}$ or $^{15}\text{N}/^{14}\text{N}$. Standards were calibrated against the international references Vienna PeeDee Belemnite for carbon and atmospheric air (N_2) for nitrogen.

Trophic level and origin of carbon

Based on the trophic position (TP) for each benthic consumer, we studied the relative assimilation and transfer of SC across the benthic community assuming a constant enrichment factor (Δ) of 2.3‰ per trophic level in consumers of aquatic environments (McCutchan et al., 2003). The surface sediment bulk $\delta^{15}\text{N}$ signature was used as a baseline in the estimation of the trophic level for each consumer. Benthic macrofauna were categorized into three different groups, high consumers (including secondary, tertiary, or upper consumers as well as scavengers, etc., $\text{TP} \geq 3$), omnivores ($3 > \text{TP} > 2$), and primary consumers ($\text{TP} \leq 2$), using Equation 4:

$$\text{TP} = \frac{\delta^{15}\text{N}_{\text{Consumer}} - \delta^{15}\text{N}_{\text{base}}}{\Delta \delta^{15}\text{N}} + \lambda, \quad \text{Equation(4)}$$

where $\delta^{15}\text{N}_{\text{Consumer}}$ is $\delta^{15}\text{N}$ of the benthic consumers, $\delta^{15}\text{N}_{\text{base}}$ is the nitrogen isotope ratio of the base of the food chain or “sediment baseline,” $\Delta \delta^{15}\text{N}$ is the trophic enrichment factor between successive trophic levels, and $\lambda = 1$ is the TP of “baseline.” The sediment baseline was estimated using the mean $\delta^{15}\text{N}$ calculated for the 17 sediment stations. Carbon isotopes ratios ($\delta^{13}\text{C}$) were used to establish the dependence of benthic macrofauna on different food sources.

SIC data

Satellite SIC data were derived from Nimbus-7 SMMR and DMSP SSM/I-SSMIS Passive Microwave Data and downloaded from the National Snow and Ice Data Center (Cavalieri et al., 1996). Spring (April 1 to June 30) SICs at each station were averaged for the period of 1998–2017, expressed in percentages, and the standard deviation (SD) was calculated. Such averaged spring SIC was considered relevant in this study because benthic consumers have access to sedimentary carbon deeper than the top approximately 1 mm deposited in 2016. Consequently, the lipid signature in animals likely represents several years of accumulated carbon.

Statistical analyses

All statistical analyses and graphical procedures were performed using R (R Core Team, 2019) and Ocean Data View version 5.1.7 (<https://odv.awi.de>), respectively. The normality of residuals was examined using Q–Q plots. Linear models were employed to evaluate simultaneously the effect of environmental variables (i.e., depth and SIC) and their interactions on percentages of SC found in both sediment and benthic consumer samples. Furthermore, linear models were used to predict the relationship between SC (%) found in sediments and SC (%) assimilated by the benthic macrofauna across stations. A cluster analysis using the Euclidean dissimilarity index was performed to identify groups and classify the benthic stations according to the relative proportion of SC assimilated by the benthic macrofauna. Box plots of the relative percentage of SC found in benthic macrofauna were made to visualize concordance with the hierarchical clustering analysis. To compare variations in the relative assimilation of SC (%) by benthic consumers across species and stations, a Tukey's test was run following an analysis of variance. Finally, using Stable Isotope Bayesian Ellipses in R (Jackson et al., 2011), standard ellipses and convex hulls were created to study interspecific ecological niche variations in the $\delta^{15}\text{N}$ versus SC iso-space. The niche space is a measure used in food web studies to describe both the amounts of resources and the habitats used by animals (Reid et al., 2016). In this context, convex hulls represent the full range of resources used by benthic consumers, whereas standard ellipses, which are bivariate equivalents of *SD*, represent the core isotopic niche, that is, resources most commonly used by consumers.

Results

Spatial distribution and relative contribution of SC in sediments

Satellite observations between the years 1998 and 2017 showed a spatial trend in the average spring SIC in the region studied (**Figure 1**). As expected, we observed more variability in SIC (**Table 1**) in the eastern region of the study area where the warmer West Greenland Current induces later ice formation and earlier ice breakup (**Figure 1A and B**). Sediment samples were comprised of four different textural groups, that is, slightly gravelly sandy mud, sandy mud, gravelly mud, and mud. The percentages of OM across all sediments ranged from 1.75% to 6.47% (**Table 1**), with no apparent relationship to textural group (linear model; $F = 4.06$, P value = 0.13), although linear models indicated that gravel ($F = 11.15$, P value < 0.01) and mud ($F = 16.62$, P value < 0.001) had an effect on OM percentage in sediment. Lower percentages of OM in sediments were recorded in the southeastern stations, while higher percentages were recorded in the western stations of Baffin Bay (**Table 1**). A linear model showed a significant effect of both depth ($F = 30.87$, P value < 0.001) and SIC ($F = 75.94$, P value < 0.001) on OM percentage in sediment, but no interactive effects between these environmental variables were detected.

HBI biomarkers indicated that all surface sediments contained both sympagic (IP₂₅, II) and pelagic (III) lipids.

In addition, the relative contribution of SC to the sediments ranged from 37% to 98% (mean SC% \pm *SD* = 86% \pm 16.0, $n = 17$; **Table 1**; **Figure S2**). Based on a linear model, SIC had a significant effect on the relative contribution of SC in sediment ($F = 118.51$, P value < 0.001), whereas no significant effects of depth alone or in combination with SIC were detected on SC. Lowest SC percentages in sediments were found in the shallower southeastern stations of Baffin Bay (**Table 1**; **Figure S2**). The greatest relative contribution of SC was encountered in the western stations of the study area, revealing a gradient of decreasing SC values from the west to the east of Baffin Bay. A similar pattern of decreasing SIC was observed from west to east in the sampled area (**Table 1**; **Figure S2**).

In addition to HBI biomarkers, Chl *a* concentrations reflected higher algal (sympagic and/or pelagic) biomass in areas with less SICs in the southeast and lower algal biomass in the west (**Table 1**). By combining OM with relative proportions of SC (sympagic vs. pelagic; H-Print), we calculated the maximum theoretical percentage value of sympagic OM (iOM) available for benthic consumption in the sediment stations sampled. This value ranged from 9% to 63% (**Table 1**). Accordingly, with maximum sedimentary OM of 6.47% (64.7 mg OM g⁻¹ dry weight) and maximum iOM content in sediment of 62.6% (based on HBI biomarker estimates), Baffin sediments could contain no more than 40 mg iOM g⁻¹ dry weight.

Relative contribution of SC to benthic macrofaunal diets

Approximately two-thirds of the benthic samples contained both sympagic (IP₂₅, II) and pelagic (III) HBIs. Regardless of the taxonomic group, benthic macrofauna showed a wide assimilation of SC (i.e., varying between 16% and 99%; mean SC% \pm *SD* = 78% \pm 19.7, $n = 159$) in most of the study area (**Table 2**). Also, the relative proportion of SC assimilated by the benthic fauna varied significantly among species ($F = 3.91$, $df = 70$, P value < 0.001) and stations ($F = 7.40$, $df = 11$, P value < .001). The lowest SC percentages were found in samples from the fish *Lumpenus lamprettaeformis* (26%), the hermit crab *Pagurus pubescens* (25%), and the sea star *Hippasteria phrygiana* (16%; **Table S1**). The brittle star *Ophiacantha bidentata* and the sea star *Pseudarchaster parelii* had the highest percentages of SC found among consumers (almost 100%).

Based on the relative proportion of SC assimilated by benthic macrofauna, a hierarchical clustering grouped benthic stations geographically into three zones (A–C; **Figure 2A**). The proportion of SC assimilated by the benthic macrofauna varied among these zones, progressively decreasing southeastward (**Figure 2B and C**). The average spring SIC ranged from 43% in the southeast to 84% in the northwest (**Figure 2C**; **Table 2**).

Based on linear models, at stations where both sediments and benthic macrofauna were sampled (**Figure 1**), a significant effect was found between SC available in sediments and SC assimilated by benthic macrofauna ($F = 33.64$, P value < 0.001). In addition, linear models

Table 1. Surface sediment data set derived from sediment stations collected in Baffin Bay in 2016. DOI: <https://doi.org/10.1525/elementa.2020.047.t1>

Station	Depth (m)	Date ^a	Latitude ^b (N)	Longitude ^b (W)	SIC ^c (%)	H-Print ^d (%)	SC ^c (%)	OM ^f (%)	iOM ^g (%)	$\delta^{13}\text{C}^h$ (‰)	$\delta^{15}\text{N}^h$ (‰)	Chl <i>a</i> ⁱ ($\mu\text{g g}^{-1}$)	Textural group ⁱ	Gravel (%)	Sand (%)	Mud (%)
G300	199 ^k	June 17, 2016	69.00	-56.79	43 ± 40	63.1	36.8	2.5	9.3	-21.3	5.1	668	SM	0.0	20.2	79.8
G418	384	June 28, 2016	68.11	-57.77	63 ± 30	40.0	60.2	1.8	10.5	-22.6	4.8	249	SGSM	0.3	44.9	54.9
G306b	309	June 18, 2016	68.99	-58.15	71 ± 30	27.6	72.9	1.8	13.0	-21.4	5.8	49	SGSM	1.5	48.3	50.2
G615	615	July 05, 2016	70.50	-59.52	76 ± 30	7.0	94.0	3.1	29.2	-21.9	7.4	61	SM	0.0	20.3	79.7
G312	1,455	June 19, 2016	69.01	-59.56	82 ± 20	10.7	90.2	5.2	46.7	-21.9	8.6	34	M	0.0	10.0	90.0
G707	1,427	July 08, 2016	69.51	-59.81	80 ± 20	12.1	88.7	4.6	40.4	-21.3	7.0	47	SM	0.0	11.5	88.5
G201	1,321	June 14, 2016	68.63	-59.95	83 ± 20	11.3	89.5	5.5	49.2	-21.8	8.0	112	SM	0.0	22.7	77.3
G409	1,407	June 26, 2016	68.11	-60.00	81 ± 20	11.0	89.8	5.2	46.6	-22.2	7.8	37	SGSM	1.4	18.6	80.0
G318	1,777	June 20, 2016	69.01	-60.95	85 ± 20	21.6	79.1	5.6	44.6	-22.7	9.4	11	GM	5.2	11.0	83.8
G115	1,719	June 13, 2016	68.46	-61.35	84 ± 20	8.0	92.9	5.1	47.2	-21.2	7.5	58	SGSM	1.2	19.1	79.8
G713	1,898	July 09, 2016	69.50	-61.58	86 ± 10	6.5	94.5	4.9	46.0	-22.2	9.6	17	GM	8.0	15.7	76.3
G403	1,675	June 25, 2016	68.03	-61.60	82 ± 20	6.6	94.3	5.0	47.6	-18.8	9.0	12	GM	6.6	13.3	80.1
G324	1,897	June 21, 2016	69.00	-62.36	85 ± 20	6.6	94.3	6.2	58.7	-21.6	8.9	15	GM	17.3	16.6	66.2
G519	2,008	July 02, 2016	70.00	-62.42	87 ± 10	6.9	94.0	5.6	52.4	-22.0	9.6	16	GM	12.8	12.4	74.8
G605	2,007	July 04, 2016	70.50	-62.52	87 ± 10	4.6	96.3	5.9	56.6	-21.8	9.8	46	SGSM	0.9	16.2	82.9
G719	1,951	July 10, 2016	69.50	-63.23	85 ± 10	4.2	96.8	6.5	62.6	-21.6	9.8	10	GM	6.4	15.0	78.7
G600	2,111	July 03, 2016	70.51	-63.99	87 ± 10	2.8	98.3	6.0	59.1	-21.9	9.3	25	GM	12.3	22.5	65.2

^aDate sampling (month/day/year).

^bSampling locations (longitudinal arrangement from east to west of Baffin Bay).

^cMean values (\pm standard deviation), average sea-ice concentration in spring between the years 1988 and 2017 ($n = 30$).

^dHighly branched isoprenoid-fingerprint or "H-Print" carbon source index (H-print > 50% is associated with pelagic carbon, and H-print < 50% is associated with SC).

^eSC = sympagic carbon.

^fOM = organic matter (percentage of sediment mass).

^giOM = ice organic matter (percentage of OM content in sediment).

^hStable isotope ratios of carbon ($\delta^{13}\text{C}$) and nitrogen ($\delta^{15}\text{N}$).

ⁱChl *a* = chlorophyll *a*.

^jSediment textural groups: slightly gravely sandy mud (SGSM), sandy mud (SM), gravely mud (GM), and mud (M).

^kThe minimum and maximum values obtained are shown in bold.

Table 2. Sampling details and trophic marker measurements in benthic macrofauna from stations collected in Baffin Bay. DOI: <https://doi.org/10.1525/elementa.2020.047.t2>

Stations	Depth (m)	Date ^a	Latitude ^b (N)	Longitude ^b (W)	SIC ^c (%)	<i>n</i> ^d	SC ^e (%)	<i>n</i> ^f	$\delta^{13}\text{C}^e$ (‰)	$\delta^{15}\text{N}^e$ (‰)
G300	199^g	June 17, 2016	69.00	-56.79	43 ± 40	12	59 ± 31.3	22	-18.1 ± 1.4	13.4 ± 1.8
G503	301	June 29, 2016	70.00	-57.76	65 ± 30	8	71 ± 10.2	20	-18.1 ± 1.3	13.5 ± 2.1
G418	384	June 28, 2016	68.11	-57.77	63 ± 30	10	61 ± 28.8	14	-18.3 ± 1.8	13.1 ± 1.2
G306b	309	June 18, 2016	68.99	-58.15	71 ± 30	8	61 ± 7.9	12	-19.4 ± 1.1	13.8 ± 2.3
G703	520	July 07, 2016	69.50	-58.72	74 ± 30	26	74 ± 19.4	36	-17.0 ± 1.9	14.7 ± 3.5
G309	360	June 18, 2016	69.00	-58.74	71 ± 30	2	78 ± 27.7	11	-18.6 ± 1.5	13.5 ± 2.2
G507	294	June 30, 2016	70.01	-59.12	77 ± 30	29	79 ± 12.5	41	-17.8 ± 1.8	13.1 ± 2.1
G107	403	June 11, 2016	68.50	-59.18	79 ± 20	4	65 ± 8.6	6	-19.7 ± 1.0	13.3 ± 2.3
G204	445	June 15, 2016	68.71	-59.26	75 ± 30	5	65 ± 23.5	12	-18.4 ± 1.3	13.9 ± 1.3
G615	615	July 05, 2016	70.50	-59.52	76 ± 30	18	88 ± 8.4	23	-17.2 ± 2.2	12.3 ± 3.2
G707	1,427	July 08, 2016	69.51	-59.81	80 ± 20	22	92 ± 5.7	31	-18.8 ± 1.7	15.0 ± 2.3
G512	605	July 01, 2016	70.00	-60.36	84 ± 20	15	94 ± 9.6	20	-18.3 ± 1.8	14.1 ± 3.3

^aDate sampling (month/day/year).

^b Sampling location (longitudinal arrangement from east to west of Baffin Bay).

^cMean value ± standard deviation (*SD*) for sea-ice concentration in spring over the years 1988–2017 (*n* = 30).

^dNumber of samples analyzed per station for sympagic carbon calculations.

^eMean values ± *SD*.

^fNumber of samples analyzed per station for stable isotope ratio analyses.

^gThe minimum and maximum values obtained are shown in bold.

indicated a significant effect of both SIC ($F = 43.21$, P value < 0.001) and depth ($F = 9.52$, P value < 0.01) and interactive effect of these environment variables ($F = 5.25$, P value < 0.05) on the SC assimilated by benthic consumers. Highest mean SC values found in benthic fauna (mean SC% ± *SD* = 94% ± 9.6, $n = 15$) were recorded at the westernmost station G512 (**Figure 2C; Table 2**).

Food web structure and transfer of SC across benthic macrofauna

HBI lipid biomarkers and $\delta^{15}\text{N}$ values of the benthic macrofauna revealed distinct niche spaces between zones (**Figure 3**). Convex hulls showed a decrease in niche width (trophic diversity) from Zones A–C. Moreover, the relative position of these hulls showed that the highest assimilation of SC by macrofauna was located in Zone C (where SC ranged between 61% and 99%; mean SC% ± *SD* = 91% ± 8.1, $n = 55$) and the lowest in Zone A (where SC ranged between 16% and 97%; mean SC% ± *SD* = 61% ± 23.7, $n = 39$). In contrast, intermediate values of SC assimilated by macrofauna were found in Zone B (where SC ranged between 54% and 99%; mean SC% ± *SD* = 76% ± 15.8, $n = 65$). Likewise, ellipses (core niche spaces) for Zones A and C showed almost no overlap, suggesting important differences in the assimilation of SC by benthic macrofauna in these regions (**Figure 3**).

Benthic macrofauna displayed a wide range of isotopic signatures (Table S1). Differences in $\delta^{15}\text{N}$ values were observed across species ($F = 18.27$, $df = 70$, P value < 0.001) and reflected in the high variability of trophic levels occupied by the consumers. Trophic markers highlighted variations in the extent of the niche space along the $\delta^{15}\text{N}$ axis between the different zones (**Figure 3**). Convex hulls and ellipses showed a trend of increasing niche length from Zones A to C, relating the shortest niche length to Zone A ($\delta^{15}\text{N}$ values from 10.7‰ to 17.9‰) and the longest to Zone C ($\delta^{15}\text{N}$ values from 6.1‰ to 20.5‰). In Zone B, $\delta^{15}\text{N}$ values ranged from 8.8‰ to 19.2‰ (**Figure 3**).

Differences in the ecological niche space across groups of benthic consumers (i.e., primary, omnivorous, and high consumers) and zones were observed (**Figure 4**). In Zone A, SC ranged from 61.6% to 72.5% in primary consumers, from 24.6% to 96.5% in omnivorous consumers, and from 16.3% to 75.8% in high consumers. In Zone B, SC ranged from 56.4% to 98.6% in primary consumers, from 54.8% to 93.2% in omnivorous consumers, and from 53.7% to 99.5% in high consumers. In Zone C, SC ranged from 85.4% to 96.7% in primary consumers, from 87.3% to 97.4% in omnivorous consumers, and from 60.6% to 99.4% in high consumers (**Figure 4**).

Likewise, the values of $\delta^{15}\text{N}$ varied across zones and consumer groups. In Zone A, $\delta^{15}\text{N}$ values ranged from 10.7‰ to 11.4‰ in primary consumers, from 12.1‰ to

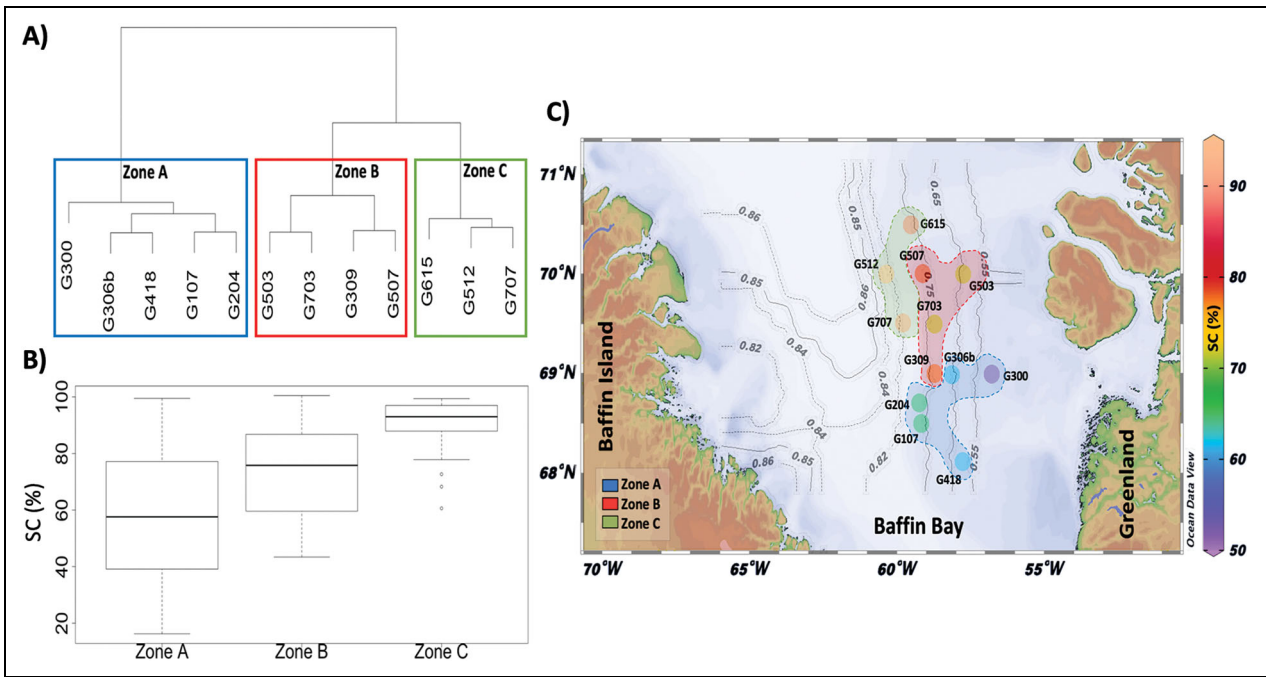


Figure 2. Cluster analysis performed on relative proportion of sympagic carbon (SC) assimilated by benthic macrofauna. Cluster analysis resulted in three different zones (A); boxplot of the relative abundance of SC assimilated by the deep benthic fauna sampled in the three zones resulting from the hierarchical clustering analysis (B); and spatial distribution and relative percentage of SC assimilated by the benthic community across the benthic stations (C). The average SIC, ranging from 0% to 100% (expressed here between 0 and 1; gray lines), derived from the National Snow and Ice Data Center in spring (April 1 to June 30) between 1998 and 2017 in Baffin Bay, Canadian Arctic. DOI: <https://doi.org/10.1525/elementa.2020.047.f2>

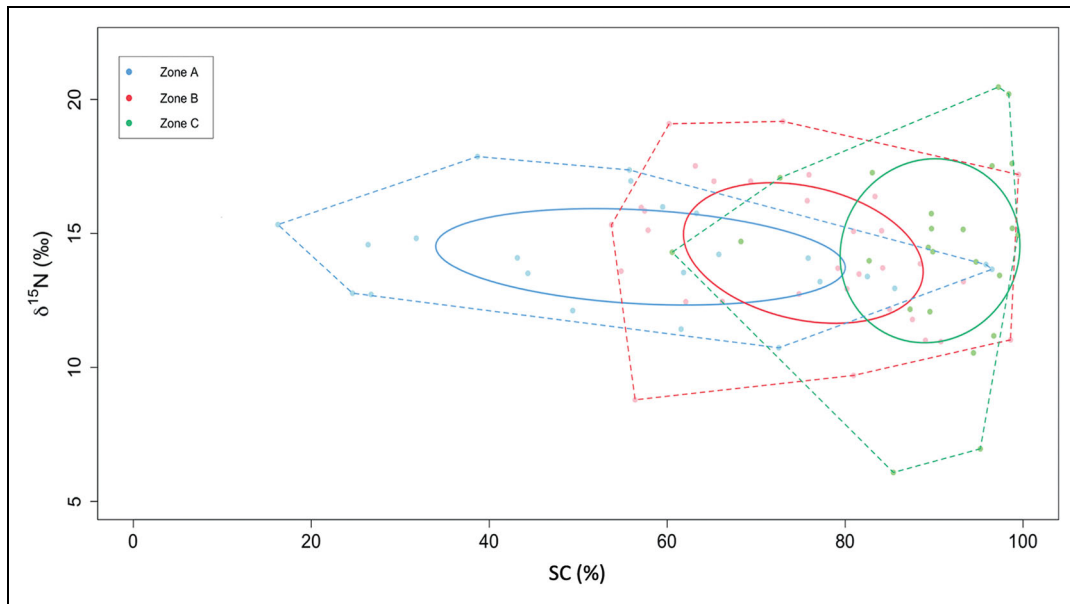


Figure 3. Biplot illustrating the ecological niche characteristics of the benthic community for each zone. Convex hulls (dashed lines) and standard ellipses (full lines) represent the niche space, sympagic carbon (SC%) versus $\delta^{15}N$, for three different zones in Baffin Bay (June 11 to July 10, 2016): Zone A (blue), Zone B (red), and Zone C (green; Figure 2). Convex hulls represent the full range of the ecological niche area of resources used by benthic consumers, while ellipses represent the core niche area used by consumers. DOI: <https://doi.org/10.1525/elementa.2020.047.f3>

13.8‰ in omnivorous consumers, and from 14.1‰ to 17.9‰ in high consumers. In Zone B, $\delta^{15}N$ values ranged from 8.8‰ to 11.0‰ in primary consumers, from 11.8‰

to 13.9‰ in omnivorous consumers, and from 15.1‰ to 19.2‰ in high consumers. Finally, in Zone C, $\delta^{15}N$ values ranged from 6.1‰ to 11.2‰ in primary consumers, from

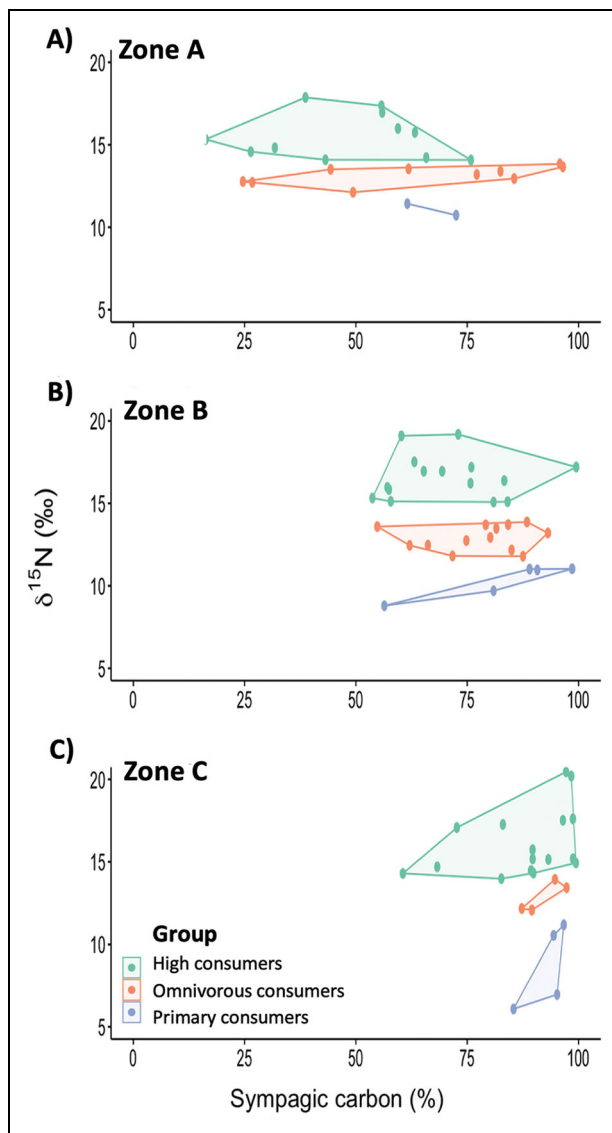


Figure 4. Biplots illustrating the ecological niche characteristics of the different benthic consumer groups. Convex hulls (full lines) represent the ecological niche space, $\delta^{15}\text{N}$ versus sympagic carbon (SC%), for three different groups of benthic consumers: high (green), omnivorous (orange), and primary (blue), in three different zones in Baffin Bay, June 11 to July 10, 2016. DOI: <https://doi.org/10.1525/elementa.2020.047.f4>

12.1‰ to 13.9‰ in omnivorous consumers, and from 14.0‰ to 20.5‰ in high consumers (Figure 4). We noted a greater variability of $\delta^{15}\text{N}$ values in both primary and high consumers in Zone C compared to the other zones.

To assess the origin of carbon, amount of resources, and habitat used by benthic macrofauna, we analyzed $\delta^{13}\text{C}$ values of consumers and food web baselines (i.e., SPOM, fresh sympagic algae, and sediment). Surface sediments were slightly enriched in carbon isotopes compared to SPOM. $\delta^{13}\text{C}$ values ranged from -23.8‰ to -20.1‰ in SPOM, from -22.7‰ to -18.8‰ in sediments, from -20.7‰ to -13.4‰ in fresh sympagic algae, and from -18.6‰ to -18.1‰ in wracks of the macroalga *Fucus vesiculosus*, found only at station G418 in Zone A.

Macrofaunal $\delta^{13}\text{C}$ values ranged from -21.5‰ to -12.9‰ . Values of $\delta^{13}\text{C}$ in benthic macrofauna ranged from -21.2‰ to -13.6‰ in Zone A, from -21.2‰ to -12.9‰ in Zone B, and from -21.5‰ to -13.7‰ in Zone C (Figure 5). Among macrofauna, the sea stars *Icasterias panopla* and *Urasterias lincki* were the most ^{13}C -enriched in this study ($\delta^{13}\text{C} = -12.9\text{‰}$ and -13.6‰ , respectively). None of the benthic macrofauna analyzed were ^{13}C -depleted to $\delta^{13}\text{C}$ values lower than -22‰ , which would have reflected a higher consumption of phytoplankton or SPOM. Differences in the shape of density distribution $\delta^{13}\text{C}$ values were observed (Figure 5), which reflect changes in relative importance of carbon sources used by consumers. The largest peak of $\delta^{13}\text{C}$ values was detected in Zone A, the second highest $\delta^{13}\text{C}$ peak in Zone B, and the lowest $\delta^{13}\text{C}$ peak in Zone C. A secondary peak of $\delta^{13}\text{C}$ was evidenced in all three zones but was more pronounced in Zone C. The $\delta^{13}\text{C}$ values from the benthic macrofauna showed similar ranges in all zones studied, but the most positive $\delta^{13}\text{C}$ values corresponded mostly to Zones B and C (Figure 5).

Discussion

Influence of SIC and depth on distribution and availability of SC in sediment

We found a significant relationship between SIC and SC, associated with a decreasing gradient in the relative contribution of SC from the western to eastern side of Baffin Bay. Our results also revealed a latitudinal SC gradient between the southeast and northwest stations, with SC increasing toward the northernmost stations. Independent of hydrographic conditions, we detected a significant effect of SIC on the relative contribution and distribution of SC in sediment. Previous studies that explored how benthic food webs responded to changes in sea ice and primary food supply highlighted the critical role that sea ice plays in Antarctic food webs (Norkko et al., 2007; Michel et al., 2019; Rossi et al., 2019). Also, lipid biomarker studies denoted how latitudinal patterns in sea-ice conditions and seasonality influenced the abundance and distribution of HBI lipids in different Arctic regions (Navarro-Rodriguez et al., 2013; Ribeiro et al., 2017; Koch et al., 2020b). In Baffin Bay, Stoyanova et al. (2013) studied the distribution of HBI lipids and observed diminishing abundances of IP₂₅ (SC proxy) in areas with less SIC toward the south of the Bay. Our data showed a similar trend, highlighting that among the studied environmental parameters, SIC has a significant effect on the relative contribution and distribution of SC on the seafloor. Therefore, changes in SIC during spring could have had a significant impact on sediment SC contents.

High SC percentages occurred at all of our stations. Previous work has shown that the abiotic degradation (e.g., Type II photodegradation and autoxidation; for a review, see Rontani and Belt, 2019) of HBI lipids increases with the number of unsaturations, and therefore, degradation rate constants of tri-unsaturated HBIs (e.g., pelagic HBI) are higher than those of the monounsaturated HBIs IP₂₅ (sympagic HBI; first-order Type II photodegradation rate constant of 1.0×10^{-2} and $1.7 \times 10^{-5} \text{ h}^{-1}$ and first-order autoxidative rate constant of 3.2×10^{-1}

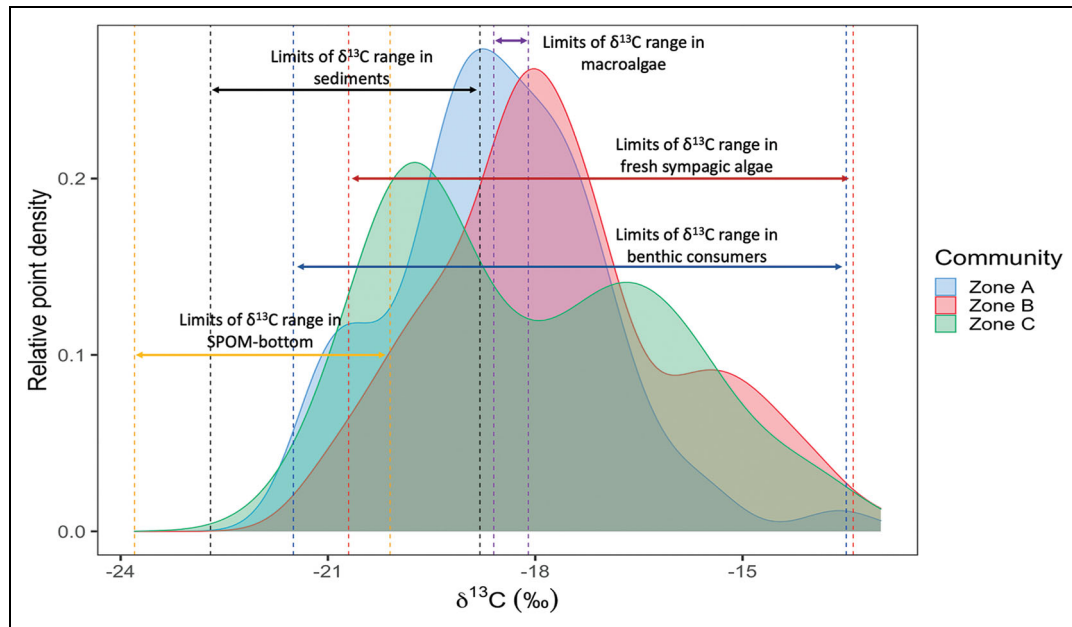


Figure 5. Density plot of $\delta^{13}\text{C}$ of the benthic community measured in Baffin Bay in spring 2016. Limits of $\delta^{13}\text{C}$ range are also shown for baseline items SPOM (yellow arrows), fresh sympagic algae (red arrows), sediment (black arrows), macroalgae (purple arrows), and benthic consumers (blue arrows). The consumer measurements are from three different zones. DOI: <https://doi.org/10.1525/elementa.2020.047.f5>

and $1.0 \times 10^{-3} \text{ h}^{-1}$ for IP₂₅ and HBI III, respectively; Rontani et al., 2011; Rontani et al., 2014). Because the calculation of SC is based on a ratio of HBI of uneven reactivity where the most subject to degradation is the pelagic HBI, degradation of OM could lead to overestimation of SC percentages. Therefore, for similar sinking rates, organic particles should experience more degradation the deeper they sink, which could cause deeper sampling sites to present higher SC percentages compared to shallower sites. However, as one of the major abiotic degradation processes (Type II photodegradation) is limited to the euphotic zone where the light necessary for this process is available (Rontani et al., 2016; Amiraux et al., 2017), the residence time of a particle within the euphotic zone should dictate its degradation rather than its travel time to sediment. Hence, for the same euphotic zone thickness, the degradation state of HBIs as well as the potential overestimation of SC between deep and shallow sampling sites should be relatively similar. Moreover, the use of pelagic and sympagic HBIs in a ratio is not a specificity of the SC percentage. The phytoplankton-IP₂₅ index (PIP₂₅; Müller et al., 2011) represents another HBI-based index based on a ratio of IP₂₅ and HBI III (Belt, 2018). By providing robust Arctic palaeo sea-ice reconstructions (Smik et al., 2016; Kim et al., 2019), this index suggests that the degradation of HBI III within the water column or sediment is reduced or at least close to that of IP₂₅. Thus, the high SC percentages observed in our deep stations should likely be derived from a relatively higher contribution of sympagic than pelagic POM rather than a preferential degradation of the pelagic biomarker. The $\delta^{13}\text{C}$ values support this interpretation, as we found the most positive $\delta^{13}\text{C}$, suggesting the strongest link with sympagic source values, in the deepest stations.

Relative contribution of SC in benthic macrofauna diets

Sea-ice lipids are known to be transferred through pelagic food webs upward to the highest trophic levels in both Arctic (Brown et al., 2017a, 2017b, 2018) and Antarctic ecosystems (Goutte et al., 2013). However, only few studies have shown the presence of HBI lipids in organisms associated with the seafloor (Brown et al., 2012; Brown and Belt, 2012; Koch et al., 2020a). Our results showed that both sea ice and pelagic HBI lipids were found in two thirds of the benthic samples analyzed. It is possible that the absence of certain HBIs (pelagic or/and sympagic) in the other third of the benthic samples could be a consequence of the tiny size of organisms, dietary preferences, rates of reactivity of HBIs, and short residence time of HBI lipids following ingestion by consumers (Koch et al., 2020a). In addition, environmental factors (e.g., nutrient availability; see Brown et al., 2020) influence the amount of HBIs produced by algae, which in turn could indirectly influence the presence or absence of HBIs in consumers. The SC quantification, combined with other trophic marker analyses, represents a novel approach to address questions related to the assimilation and transfer of HBI lipids through the benthic food web. However, more studies using this approach are necessary to conclude how biological, environmental, and chemical processes could affect their detection in sediment and organisms.

Even if the assimilated contributions of SC varied between species present at each station, the average SC (%) found in sediments and SC (%) assimilated by benthic macrofauna across stations did not differ notably. This suggests that the relative abundance of SC assimilated in spring by benthic consumers could be explained partly by the relative abundance of SC available on the seabed

(Tables 1 and 2), although benthic consumer identity (i.e., taxonomic group) or feeding strategy (i.e., functional group) could also play a role (see below). Consumption pathways of OM across the benthic community have been documented previously in the Arctic (Hobson et al., 2002; McTigue and Dunton, 2014; Mäkelä et al., 2017), showing variations in the utilization of phytoplankton or SC sources across regions and time. However, studies that investigated the role of sea-ice-derived carbon in benthic diets during spring indicated that SC and bacterially reworked OM represented the most important food sources for benthic consumers (North et al., 2014; Kohlbach et al., 2019). Regardless of how we addressed the analysis of the carbon assimilation and transfer through benthic consumers (i.e., HBI and/or stable isotope analyses), the spread of values showed similar results, among which benthic consumers exhibited strong patterns in SC assimilation in response to gradients of SC values. Hence, SC (%) assimilated by deep benthic fauna increased toward sites with higher SIC during the spring in the northwest of Baffin Bay. Based on our results, we highlight SC as an important food source in the diet of different benthic taxa in springtime.

Food web structure and transfer of SC

Trophic markers revealed shifts in the ecological niche space (i.e., niche width) of the benthic community across zones. Decreases in niche width from Zones A to C suggested a greater diversity of carbon sources used by consumers in Zone A. Our results showed that the percentage of SC available for benthic consumption is a determining factor shaping the ecological niche space. Thus, the most significant differences in niche space corresponded to areas with strong differences in SC percentages (**Figure 3**). Across trophic groups, changes in the niche space revealed variations in SC assimilation by benthic macrofauna. Omnivorous and primary consumers relied the most on SC in all zones, showing the narrowest niche space in Zone C. On the other hand, high consumers showed low to moderate assimilation of SC in Zone A, with a high increase in SC assimilation in Zones B and C. In addition to variations in the niche width, $\delta^{15}\text{N}$ range was greater in both primary and high consumers from Zone C, compared to Zones A and B. Although percentages of SC available for the consumption of benthic macrofauna should vary over the seasons and regions (Boetius et al., 2013), benthic consumers can specialize on the consumption of some available basal resources, which is ultimately reflected in the food web structure (Rossi et al., 2019). Likewise, changes in the ecological niche can reflect mechanisms adopted by the different groups to ingest different food sources (Iken et al., 2001). For example, primary consumers adapted to feed on more selective food items occupied a restricted ecological niche space and the lowest TPs in this study. This result means that aside from environmental conditions that influence the availability of food sources, changes in the benthic food web could be a reflection of the plasticity of those benthic consumers that can ingest different carbon sources efficiently (Mäkelä et al., 2017). For instance, *Rossia megaptera*, a cephalopod,

shifted from a high trophic level in Zone A (high consumers) to a lower trophic level (omnivorous) in Zone B. In addition, our data suggest that high availability of SC may influence the transfer efficiency of this basal source.

The $\delta^{13}\text{C}$ values from the benthic community revealed differences in resource assimilation between zones, indicating that consumers probably depend on multiple baseline items, among which sympagic algae provide one of the main carbon inputs for consumers in spring. Very positive $\delta^{13}\text{C}$ values (typically linked to consumption of ice algae) were found mainly in benthic fauna from Zones B and C, suggesting that at the time of sampling, the SC resource might be used less commonly by benthic fauna in Zone A (**Figure 5**). Some studies have proposed a link between ^{13}C -enriched benthic invertebrates and the consumption of organic material that has been reworked by microbes (Michel et al., 2016; Amaro et al., 2019; Gradinger and Bluhm, 2020). Therefore, unaccounted resources (e.g., from bacteria) may have also influenced isotopic compositions in consumers. Likewise, increases of $\delta^{15}\text{N}$ with depth in both sediments and benthic fauna may be linked to biological and chemical processes, including microbial consumption and degradation of OM in the water column (Macko and Estep, 1984; Stasko et al., 2018) and remineralization (Feder et al., 2011; Lehmann et al., 2019), which could influence nitrogen isotopic compositions across benthic macrofauna. However, for some surface deposit feeders (e.g., the arthropod *Diastylis rathkei*), we found exceptionally low $\delta^{15}\text{N}$ values (at the same level of the baseline/sediment $\delta^{15}\text{N}$ values), coinciding with previous findings (Iken et al., 2005; Renaud et al., 2011). The cause for these depleted ^{15}N values remains unexplained in this study, but ^{15}N depletions may have been influenced by the isotopic composition of unknown baseline sources such as cyanobacteria or other N_2 -fixing microorganisms (Karlson et al., 2014). Based on our results, the benthic food web is supported by several carbon sources. In springtime, however, sympagic algae and probably microbially degraded OM seem to have important functions in supporting and shaping the benthic food web. Although this study gives some clues about the functioning of the benthic food web, many questions remain to be resolved, including the role of microbial communities in deep benthic food webs. Continued study of how temporal and spatial changes in basal resource inputs, including reworked material, impact nutrient transfer and food web structure is needed, particularly in areas with notable changes in SIC.

Climate change, consumer diets, and food web structure

The quantity of POC that reaches the polar seabed influences deep benthic community structure and plays an essential role in shaping patterns and trends in biomass, density, and macrobenthic production (Grebmeier and Barry, 1991; Degen et al., 2015). Coinciding with reductions in sea-ice cover and warming waters, shifts in both benthic biomass and species composition have been described for some Arctic regions, suggesting that climate change may also impact biological diversity in these deep-

sea ecosystems (Grebmeier et al., 2018; Rybakova et al., 2019). Predictions point to future alterations in primary production in the Arctic Ocean due to a reduction in sea-ice extent and changes in its phenology (Tedesco et al., 2019). As a result, the quality and quantity of the OM that reaches the seafloor will be impacted negatively by taxonomic and biochemical alterations and by increased grazing pressure in the pelagic zone (Jeffreys et al., 2013), which could in turn weaken pelagic-benthic coupling processes (Olivier et al., 2020) and the efficiency of energy transfers across food webs (Post, 2017). In terms of food quality, Leu et al. (2011) found that sympagic primary production is generally of better nutritional quality than pelagic production. Moreover, sympagic production is better conserved because of its higher sinking rates (avoiding most of the abiotic degradation that occurs in euphotic zones) and frequent mismatch with the onset of grazing activity. Hence, an increase in phytoplankton production due to an earlier onset of sea-ice melt will not necessarily imply more food for deep benthic communities. Instead, climate change may reduce the size of phytoplanktonic cells (Li et al., 2009) and lower the overall quality and quantity of some primary food sources. Here, we established a connection between contrasting sea-ice conditions and changes in deep benthic consumer diets and food web structure. Our results denoted a link between niche sizes and diversity of food sources, highlighting a reduction in niche size when food diversity decreased. As an increase in the diversity of basal sources leads to temporal stability in the supply of organic carbon to food webs, food restrictions (i.e., decrease in diversity) could lead to the temporal instability of the system (Wing et al., 2012). Likewise, preference for ice algae as food was reflected in niche sizes. Narrower niches were associated with primary and omnivorous consumers in regions with a major abundance of SC. Consumer food preferences may be linked to feeding mode and the ability of animals to capture, handle, and digest food and to the energy value that this resource represents for consumers (Araújo et al., 2011). Thus, instead of revealing lesser adaptability to ingest different kinds of food sources, narrow niches may reflect the strategies adopted by consumers to ingest food of great nutritional value. Finally, ellipses and $\delta^{13}\text{C}$ values indicated that the resource most commonly used by consumers was ice algae. A reduction in the availability of SC could increase both intraspecific and interspecific competition and predation among the consumers, ultimately affecting structure, dynamics, and seasonal stability of deep-sea benthic food webs in the Canadian Arctic.

Conclusions

Quantifying the importance of SC as a food source in the Arctic is an increasingly important research objective as sea-ice extent and thickness continue to decline. The present study represents the first analysis of the transfer of sea-ice and pelagic lipids through a diverse range of benthic species at different depths and sea-ice conditions, supporting the idea that SC is an important energy subsidy for deep benthic communities that could be disrupted in the years to come. Climate change will drive

food quality and availability in the future Arctic Ocean, which can affect the transfer of matter and energy to high-level consumers, including commercial fish and Inuit people. Also, a greater disparity in the formation and melting period of sea ice could lead to consequences not yet defined in cycles of production and delivery of OM to benthic fauna. Changes in the quantity of sympagic OM available to benthic consumers and/or the timing of its availability could disrupt the life cycles of benthic organisms and affect lower benthic trophic levels. Such disruption could in turn induce changes in ecosystem functioning at different levels in the Arctic food web. The use of lipid biomarkers in the quantification of SC assimilated by benthic consumers proved to be a powerful technique that could enhance our understanding of deep benthic communities. Also, the novel combination of HBLs with stable isotope ratios ($\delta^{15}\text{N}$; $\delta^{13}\text{C}$) was shown to be a suitable method in the study of the benthic food web structure. Our results indicated considerable assimilation of SC by benthic consumers during spring/early summer, providing estimates of SC assimilated by benthic consumers in areas with different dynamics in sea-ice cover. Regardless of depth, our results showed that the relative contribution and distribution of SC in the seabed was regulated mainly by sea-ice cover. In this study, availability of food sources and ecological strategies (i.e., diversity of resources and habitats used by animals) adopted by benthic consumers were major drivers shaping the benthic food web structure across sampled sites. As benthic fauna are key members of the organic carbon cycle, further long-term studies encompassing all four seasons over multiple years would be beneficial to establishing how variations in sea-ice phenology can influence food supply and nutrient transfers among Arctic benthos. Decreases in spring SICs with alterations in timing, quantity, and origins of the OM that reach the seafloor could lead to temporal changes in the nutritional composition of benthic consumer diets, which in turn could impact the structure and functioning of these ecosystems. In response to Arctic warming, raising our capacity to detect the ecological impacts of continued sea-ice decline is a fundamental priority, requiring more empirical studies that explicitly test the effects of sea-ice reduction on biological responses and the resilience of the ecosystem.

Data accessibility statement

The species data sets generated and/or analyzed during the current study are included in this article (Supplemental files). Additional data sets, including highly branched isoprenoid values used to calculate H-Print and sympagic carbon in deep-sea benthic macrofauna, are accessible in the Green Edge database (<http://www.obs-vlfr.fr/proof/php/GREENEDGE/greenedge.php>).

Supplemental files

The supplemental files for this article can be found as follows:

Figure S1. Molecular structures of highly branched isoprenoid alkenes measured in this study.

Figure S2. Sediment stations showing the spatial distribution and relative percentage of sympagic carbon in Baffin Bay.

Table S1. Benthic macrofauna measurements from samples collected in Baffin Bay in spring 2016.

Acknowledgments

Our sincere thanks to the Green Edge project (<http://www.greenedgeproject.info>) for providing us with the financial resources to make this research possible. We also thank Sentinel North and Québec-Océan for providing financial resources for training purposes. We wish to thank officers and the crew of the Canadian research icebreaker CCGS *Amundsen* for providing the support and facilities during the oceanographic campaign of 2016 in the Arctic. We also express our gratitude to Cindy Grant and the sampling team Katrine Chalut and Noémie Pelletier for their great work in the field campaign. Likewise, we thank the research professionals Laure de Montety, Lisa Treau de Coeli, and Caroline Guilmette for the help with the benthos and Geochemistry lab. We are thankful to Laval University, Takuvik, ArcticNet, and Québec-Océan for their contribution in terms of logistic, equipment, and facilities. A special recognition to the Scottish Association for Marine Science for providing us with their facilities for processing a portion of the samples analyzed in this research. The lead author warmly thanks Eric Rehm, Philippe Massicotte, and Jang Han Lee for their help with R and Ocean Data view software. Finally, the lead author expresses gratitude to Karen Filbee-Dexter for contributing ideas and feedback, Flavienne Bruyant for her help in pigment analysis, and Sergio Cortez Ghio for his help and valuable comments about the statistical analyses carried out throughout this investigation.

Funding

The Green Edge project is funded by the following French and Canadian programs and agencies: ANR (Contract #111112), CNES (project #131425), IPEV (project #1164), CSA, Foundation Total, ArcticNet, LEFE, and the French Arctic Initiative (Green Edge project).

Competing interests

Authors declare no competing interests.

Author contributions

Contributed to conception and design: GY-G, PA, CN.

Identification and separation of samples: GY-G.

Methodology highly branched isoprenoids (HBIs): TAB.

Lipids extraction and analyses: GY-G, TAB.

Stable isotope data analyses: GY-G and LNM.

HBI data analysis: GY-G, TAB, LNM.

Figures: GY-G, LNM.

Writing original draft: GY-G.

Drafted and/or revised this article: GY-G, TAB, CN, LNM, BS-B, RA, PA.

Approved the submitted version for publication: GY-G, TAB, CN, LNM, BS-B, RA, PA.

References

- Arctic Monitoring and Assessment Programme.** 2018. Adaptation Actions for a Changing Arctic: Perspectives from the Baffin Bay/Davis Strait Region. Arctic Monitoring and Assessment Programme (AMAP), Oslo, Norway. xvi + 354 pp.
- Amaro, T, Danovaro, R, Matsui, Y, Rastelli, E, Wolff, GA, Nomaki, H.** 2019. Possible links between holothurian lipid compositions and differences in organic matter (OM) supply at the western Pacific abyssal plains. *Deep Res Part I* **152**. DOI: <http://dx.doi.org/10.1016/j.dsr.2019.103085>.
- Amiriaux, R, Belt, ST, Vaultier, F, Galindo, V, Gosselin, M, Bonin, P, Rontani, JF.** 2017. Monitoring photo-oxidative and salinity-induced bacterial stress in the Canadian Arctic using specific lipid tracers. *Mar Chem* **194**: 89–99. DOI: <http://dx.doi.org/10.1016/j.marchem.2017.05.006>.
- Araújo, MS, Bolnick, DI, Layman, CA.** 2011. The ecological causes of individual specialisation. *Ecol Lett* **14**(9): 948–958. DOI: <http://dx.doi.org/10.1111/j.1461-0248.2011.01662.x>.
- Belt, ST, Brown, TA, Rodriguez, AN, Sanz, PC, Tonkin, A, Ingle, R.** 2012. A reproducible method for the extraction, identification and quantification of the Arctic sea ice proxy IP₂₅ from marine sediments. *Anal Methods* **4**(3): 705–713. DOI: <http://dx.doi.org/10.1039/c2ay05728j>.
- Belt, ST.** 2018. Source-specific biomarkers as proxies for Arctic and Antarctic sea ice. *Org Geochem* **125**: 277–298. DOI: <http://dx.doi.org/10.1016/j.orggeochem.2018.10.002>.
- Belt, ST, Massé, G, Rowland, SJ, Poulin, M, Michel, C, LeBlanc, B.** 2007. A novel chemical fossil of palaeo sea ice: IP₂₅. *Org Geochem* **38**(1): 16–27. DOI: <http://dx.doi.org/10.1016/j.orggeochem.2006.09.013>.
- Belt, ST, Smik, L, Köseo, D, Knies, J, Husum, K.** 2019. A novel biomarker-based proxy for the spring phytoplankton bloom in Arctic and sub-arctic settings—HBI T₂₅. *Earth Planet Sci Lett* **523**. DOI: <http://dx.doi.org/10.1016/j.epsl.2019.06.038>.
- Bi, H, Zhang, Z, Wang, Y, Xu, X, Liang, Y, Huang, J, Liu, Y, Fu, M.** 2019. Baffin Bay sea ice inflow and outflow: 1978–1979 to 2016–2017. *Cryosph* **13**: 1025–1042.
- Bluhm, BA, Ambrose, WG, Bergmann, M, Clough, LM, Gebruk, AV, Hasemann, C, Iken, K, Klages, M, MacDonald, IR, Renaud, PE, Schewe, I, Soltwedel, T, Włodarska-Kowalczyk, M.** 2011. Diversity of the arctic deep-sea benthos. *Mar Biodivers* **41**(1): 87–107. DOI: <http://dx.doi.org/10.1007/s12526-010-0078-4>.
- Boetius, A, Albrecht, S, Bakker, K, Bienhold, C, Felden, J, Fernández-Méndez, M, Hendricks, S, Katlein, C, Lalande, C, Krumpfen, T, Nicolaus, M, Peeken, I, Rabe, B, Rogacheva, A, Rybakova, E, Somavilla, R, Wenzhöfer, F, Polarstern, RV.** 2013. Export of algal biomass from the melting arctic sea ice. *Science* **339**(6126): 1430–1432. DOI: <http://dx.doi.org/10.1126/science.1231346>.

- Brown, TA, Assmy, P, Hop, H, Wold, A, Belt, ST.** 2017a. Transfer of ice algae carbon to ice-associated amphipods in the high-Arctic pack ice environment. *J Plankton Res* **39**(4): 664–674. DOI: <http://dx.doi.org/10.1093/plankt/fbx030>.
- Brown, TA, Belt, ST.** 2012. Identification of the sea ice diatom biomarker IP₂₅ in Arctic benthic macrofauna: Direct evidence for a sea ice diatom diet in Arctic heterotrophs. *Polar Biol* **35**(1): 131–137. DOI: <http://dx.doi.org/10.1007/s00300-011-1045-7>.
- Brown, TA, Belt, ST.** 2016. Novel tri- and tetra-unsaturated highly branched isoprenoid (HBI) alkenes from the marine diatom *Pleurosigma* intermediate. *Org Geochem* **91**: 120–122. Elsevier Ltd. DOI: <http://dx.doi.org/10.1016/j.orggeochem.2015.11.008>.
- Brown, TA, Belt, ST.** 2017. Biomarker-based H-Print quantifies the composition of mixed sympagic and pelagic algae consumed by *Artemia* sp. *J Exp Mar Bio Ecol* **488**: 32–37. DOI: <http://dx.doi.org/10.1016/j.jembe.2016.12.007>.
- Brown, TA, Belt, ST, Gosselin, M, Levasseur, M, Poulin, M, Mundy, CJ.** 2016. Quantitative estimates of sinking sea ice particulate organic carbon based on the biomarker IP₂₅. *Mar Ecol Prog Ser* **546**: 17–29. DOI: <http://dx.doi.org/10.3354/meps11668>.
- Brown, TA, Belt, ST, Piepenburg, D.** 2012. Evidence for a pan-Arctic sea-ice diatom diet in *Strongylocentrotus* spp. *Polar Biol* **35**(8): 1281–1287. DOI: <http://dx.doi.org/10.1007/s00300-012-1164-9>.
- Brown, TA, Chrystal, E, Ferguson, SH, Yurkowski, DJ, Watt, C, Hussey, NE, Kelley, TC, Belt, ST.** 2017b. Coupled changes between the H-Print biomarker and $\delta^{15}\text{N}$ indicates a variable sea ice carbon contribution to the diet of Cumberland Sound beluga whales. *Limnol Oceanogr* **62**(4): 1606–1619. DOI: <http://dx.doi.org/10.1002/lno.10520>.
- Brown, TA, Galicia, MP, Thiemann, GW, Belt, ST, Yurkowski, DJ, Dyck, MG.** 2018. High contributions of sea ice derived carbon in polar bear (*Ursus maritimus*) tissue. *PLoS One* **13**(1): 1–13. DOI: <http://dx.doi.org/10.1371/journal.pone.0191631>.
- Brown, TA, Hegseth, EN, Belt, ST.** 2013. A biomarker-based investigation of the mid-winter ecosystem in Rjippfjorden, Svalbard. *Polar Biol* **38**(1): 37–50. DOI: <http://dx.doi.org/10.1007/s00300-013-1352-2>.
- Brown, TA, Rad-Menéndez, C, Ray, JL, Skaar, KS, Thomas, N, Ruiz-Gonzales, C, Leu, E.** 2020. Influence of nutrient availability on Arctic sea ice diatom HBI lipid synthesis. *Org Geochem* **141**: 103977. <https://doi.org/10.1016/j.orggeochem.2020.103977>.
- Brown, TA, Yurkowski, DJ, Ferguson, SH, Alexander, C, Belt, ST.** 2014. H-Print: A new chemical fingerprinting approach for distinguishing primary production sources in Arctic ecosystems. *Environ Chem Lett* **12**(3): 387–392. DOI: <http://dx.doi.org/10.1007/s10311-014-0459-1>.
- Budge, SM, Wooller, MJ, Springer, AM, Iverson, SJ, McRoy, CP, Divoky, GJ.** 2008. Tracing carbon flow in an arctic marine food web using fatty acid-stable isotope analysis. *Oecologia* **157**: 117–129. DOI: <http://dx.doi.org/10.1007/s00442-008-1053-7>.
- Calizza, E, Careddu, G, Sporta Caputi, S, Rossi, L, Costantini, ML.** 2018. Time- and depth-wise trophic niche shifts in Antarctic benthos. *PLoS One* **13**(3): 1–17. DOI: <http://dx.doi.org/10.1371/journal.pone.0194796>.
- Cavaliere, DJ, Parkinson, CL, Gloersen, P, Zwally, HJ.** 1996. Sea Ice Concentrations from Nimbus-7 SMMR and DMSP SSM/I-SSMIS Passive Microwave Data, Version 1, Boulder, Color., USA. NASA National Snow and Ice Data Center Distributed Active Archive Center. DOI: <https://doi.org/10.5067/8GQ8LZQVL0VL>.
- Collin, A, Archambault, P, Long, B.** 2011. Predicting species diversity of benthic communities within turbid nearshore using full-waveform bathymetric LiDAR and machine learners. *PLoS One* **6**(6). DOI: <http://dx.doi.org/10.1371/journal.pone.0021265>.
- Degen, R, Vedenin, A, Gusky, M, Boetius, A, Brey, T.** 2015. Patterns and trends of macrobenthic abundance, biomass and production in the deep Arctic Ocean. *Polar Res* **34**(1): 24008. DOI: <http://dx.doi.org/10.3402/polar.v34.24008>.
- Divine, LM, Iken, K, Bluhm, BA.** 2015. Regional benthic food web structure on the Alaska Beaufort Sea shelf. *Mar Ecol Prog Ser* **531**: 15–32. DOI: <http://dx.doi.org/10.3354/meps11340>.
- Environment and Climate Change Canada.** 2019. Canadian Environmental Sustainability Indicators: Sea ice in Canada. Available at: www.canada.ca/en/environment-climate-change/services/environmental-indicators/sea-ice.html.
- Feder, HM, Iken, K, Blanchard, AL, Jewett, SC, Schonberg, S.** 2011. Benthic food web structure in the southeastern Chukchi Sea: An assessment using $\delta^{13}\text{C}$ and $\delta^{15}\text{N}$ analyses. *Polar Biol* **34**(4): 521–532. DOI: <http://dx.doi.org/10.1007/s00300-010-0906-9>.
- Findlay, HS, Gibson, G, Kedra, M, Morata, N, Orchowska, M, Pavlov, AK, Reigstad, M, Silyakova, A, Tremblay, JÉ, Walczowski, W, Weydmann, A, Logvinova, C.** 2015. Responses in Arctic marine carbon cycle processes: Conceptual scenarios and implications for ecosystem function. *Polar Res* **34**(2015). DOI: <http://dx.doi.org/10.3402/polar.v34.24252>.
- Frey, KE, Comiso, JC, Cooper, LW, Grebmeier, JM, Stock, LV.** 2018. Arctic Ocean primary productivity: The response of marine algae to climate warming and sea ice decline. Arctic Report Card 2018. Available at <https://www.arctic.noaa.gov/Report-Card>.
- Gage, JD.** 2003. Food inputs, utilization, carbon flow and energetic, in Tyler, PA ed., *Ecosystems of the deep oceans*. New York, NY: Elsevier: 313–380 (Ecosystems of the World).
- Glover, AG, Gooday, AJ, Bailey, DM, Billett, DSM, Chevaldonné, P, Colaço, A, Copley, J, Cuvelier, D, Desbruyères, D, Kalogeropoulou, V, Klages, M, Lampadariou, N, Lejeune, C, Mestre, NC,**

- Paterson, GLJ, Perez, T, Ruhl, H, Sarrazin, J, Soltwedel, T, Soto, EH, Thatje, S, Tselepidis, A, Van Gaever, S, Vanreusel, A. 2010. Temporal change in deep-sea benthic ecosystems. A review of the evidence from recent time-series studies. *Adv Mar Biol* **58**(C): 1–95. DOI: <http://dx.doi.org/10.1016/B978-0-12-381015-1.00001-0>.
- Gosselin, M, Lavoie, M, Wheeler, PA, Horner, RA, Booth, BC. 1997. New measurements of phytoplankton and ice algal production in the Arctic Ocean. *Deep Res Part II* **44**(8): 1623–1644.
- Goutte, A, Chereil, Y, Houssais, MN, Klein, V, Ozouf-Costaz, C, Raccurt, M, Robineau, C, Massé, G. 2013. Diatom-specific highly branched isoprenoids as biomarkers in Antarctic consumers. *PLoS One* **8**(2). DOI: <http://dx.doi.org/10.1371/journal.pone.0056504>.
- Gradinger, R, Bluhm, B. 2020. First Arctic sea ice meiofauna food web analysis based on abundance, biomass and stable isotope ratios of sea ice metazoan fauna from near-shore Arctic fast ice. *Mar Ecol Prog Ser* **634**: 29–43. DOI: <http://dx.doi.org/10.3354/meps13170>.
- Grebmeier, JM, Barry, JP. 1991. The influence of oceanographic processes on pelagic-benthic coupling in polar regions: A benthic perspective. *J Mar Syst* **2**(3–4): 495–518. DOI: [http://dx.doi.org/10.1016/0924-7963\(91\)90049-Z](http://dx.doi.org/10.1016/0924-7963(91)90049-Z).
- Grebmeier, JM, Frey, KE, Cooper, LW, Kędra, M. 2018. Trends in benthic macrofaunal populations, seasonal sea ice persistence, and bottom water temperatures in the Bering Strait region. *Oceanography* **31**(2):136–151. DOI: <https://doi.org/10.5670/oceanog.2018.224>.
- Griffiths, JR, Kadin, M, Nascimento, FJA, Tamelander, T, Törnroos, A, Bonaglia, S, Bonsdorff, E, Brüchert, V, Gårdmark, A, Järnström, M, Kotta, J, Lindegren, M, Nordström, MC, Norkko, A, Olsson, J, Weigel, B, Žydelis, R, Blenckner, T, Niiranen, S, Winder, M. 2017. The importance of benthic–pelagic coupling for marine ecosystem functioning in a changing world. *Glob Chang Biol* **23**(6): 2179–2196. DOI: <http://dx.doi.org/10.1111/gcb.13642>.
- Hobson, KA, Fisk, A, Karnovsky, N, Holst, M, Gagnon, J-M, Fortier, M. 2002. A stable isotope ($\delta^{13}\text{C}$, $\delta^{15}\text{N}$) model for the North Water food web: implications for evaluating trophodynamics and the flow of energy and contaminants. *Deep Sea Res Part II* **49**(22): 5131–5150.
- Iken, K, Bluhm, BA, Gradinger, R. 2005. Food web structure in the high Arctic Canada Basin: Evidence from $\delta^{13}\text{C}$ and $\delta^{15}\text{N}$ analysis. *Polar Biol* **28**(3): 238–249. DOI: <http://dx.doi.org/10.1007/s00300-004-0669-2>.
- Iken, K, Brey, T, Wand, U, Voigt, J, Junghans, P. 2001. Food web structure of the benthic community at the Porcupine Abyssal Plain (NE Atlantic): A stable isotope analysis. *Prog Oceanogr* **50**(1–4): 383–405. DOI: [http://dx.doi.org/10.1016/S0079-6611\(01\)00062-3](http://dx.doi.org/10.1016/S0079-6611(01)00062-3).
- Jackson, AL, Inger, R, Parnell, AC, Bearhop, S. 2011. Comparing isotopic niche widths among and within communities: SIBER - Stable Isotope Bayesian Ellipses in R. *J Anim Ecol* **80**(3): 595–602. DOI: <http://dx.doi.org/10.1111/j.1365-2656.2011.01806.x>.
- Jeffreys, RM, Burke, C, Jamieson, AJ, Narayanaswamy, BE, Ruhl, HA, Smith, KL, Witte, U. 2013. Feeding preferences of abyssal macrofauna inferred from in situ pulse chase experiments. *PLoS One* **8**(11): 1–15. DOI: <http://dx.doi.org/10.1371/journal.pone.0080510>.
- Karlson, AML, Gorokhova, E, Elmgren, R. 2014. Nitrogen fixed by cyanobacteria is utilized by deposit-feeders. *PLoS One* **9**(8). DOI: <http://dx.doi.org/10.1371/journal.pone.0104460>.
- Kędra, M, Moritz, C, Choy, ES, David, C, Degen, R, Duerksen, S, Ellingsen, I, Górska, B, Grebmeier, JM, Kirievskaya, D, van Oevelen, D, Piwosz, K, Samuelsen, A, Węśławski, JM. 2015. Status and trends in the structure of Arctic benthic food webs. *Polar Res* **34**(2015). DOI: <http://dx.doi.org/10.3402/polar.v34.23775>.
- Kelly, JR, Scheibling, RE. 2012. Fatty acids as dietary tracers in benthic food webs. *Mar Ecol Prog Ser* **446**: 1–22. DOI: <http://dx.doi.org/10.3354/meps09559>.
- Kim, JH, Gal, JK, Jun, SY, Smik, L, Kim, D, Belt, ST, Park, K, Shin, KH, Nam, S II. 2019. Reconstructing spring sea ice concentration in the Chukchi Sea over recent centuries: Insights into the application of the PIP₂₅ index. *Environ Res Lett* **14**(12). DOI: <http://dx.doi.org/10.1088/1748-9326/ab4b6e>.
- Koch, CW, Cooper, LW, Grebmeier, JM, Frey, K, Brown, TA. 2020a. Ice algae resource utilization by benthic macro- and megafaunal communities on the Pacific Arctic shelf determined through lipid biomarker analysis. *Mar Ecol Prog Ser* **651**: 23–43. DOI: <http://dx.doi.org/10.3354/meps13476>.
- Koch, CW, Cooper, LW, Lalande, C, Brown, TA, Frey, KE, Grebmeier, JM. 2020b. Seasonal and latitudinal variations in sea ice algae deposition in the northern Bering and Chukchi seas determined by algal biomarkers. *PLoS One* **15**. DOI: <http://dx.doi.org/10.1371/journal.pone.0231178>.
- Kohlbach, D, Ferguson, SH, Brown, TA, Michel, C. 2019. Landfast sea ice–benthic coupling during spring and potential impacts of system changes on food web dynamics in Eclipse Sound, Canadian Arctic. *Mar Ecol Prog Ser* **627**: 33–48. DOI: <http://dx.doi.org/10.3354/meps13071>.
- Layman, CA, Allgeier, JE. 2012. Characterizing trophic ecology of generalist consumers: A case study of the invasive lionfish in the Bahamas. *Mar Ecol Prog Ser* **448**: 131–141. DOI: <http://dx.doi.org/10.3354/meps09511>.
- Layman, CA, Arrington, DA, Montaña, CG, Post, DM. 2007. Can stable isotope ratios provide for community-wide measures of trophic structure? *Ecology* **89**(8): 2358–2359. DOI: <http://dx.doi.org/10.1890/08-0167.1>.

- Lehmann, N, Kienast, M, Granger, J, Bourbonnais, A, Altabet, MA, Tremblay, J.** 2019. Remote western Arctic nutrients fuel remineralization in deep Baffin Bay. *Glob Biogeochem Cy* **33**(6): 649–667. DOI: <http://dx.doi.org/10.1029/2018GB006134>.
- Leu, E, Brown, TA, Graeve, M, Wiktor, J, Hoppe, JM, Chierici, M, Fransson, A, Verbiest, S, Kvernvik, AC, Greenacre, MJ.** 2020. Spatial and temporal variability of ice algal trophic markers—with recommendations about their application. *Mar Sci Eng* **8**(9), 676. doi:10.3390/jmse8090676.
- Leu, E, Søreide, JE, Hessen, DO, Falk-Petersen, S, Berge, J.** 2011. Consequences of changing sea-ice cover for primary and secondary producers in the European Arctic shelf seas: Timing, quantity, and quality. *Prog Oceanogr* **90**(1–4): 18–32. DOI: <http://dx.doi.org/10.1016/j.pocean.2011.02.004>.
- Li, KW, McLaughlin, FA, Lovejoy, C, Carmack, EC.** 2009. Smallest algae thrive as the Arctic Ocean freshens. *Science* **326**. DOI: <http://dx.doi.org/10.1126/science.1179798>.
- Link, H, Archambault, P, Tamelander, T, Renaud, PE, Piepenburg, D.** 2011. Spring-to-summer changes and regional variability of benthic processes in the western Canadian Arctic. *Polar Biol* **34**(12): 2025–2038. DOI: <http://dx.doi.org/10.1007/s00300-011-1046-6>.
- Macko, SA, Estep, MLF.** 1984. Microbial alteration of stable nitrogen and carbon isotopic compositions of organic matter. *Org Geochem* **6**(C): 787–790. DOI: [http://dx.doi.org/10.1016/0146-6380\(84\)90100-1](http://dx.doi.org/10.1016/0146-6380(84)90100-1).
- Mäkelä, A, Witte, U, Archambault, P.** 2017. Ice algae versus phytoplankton: Resource utilization by Arctic deep sea macroinfauna revealed through isotope labelling experiments. *Mar Ecol Prog Ser* **572**: 1–18. DOI: <http://dx.doi.org/10.3354/meps12157>.
- McCutchan, JH, Lewis, WM, Kendall, C, McGrath, CC.** 2003. Variation in trophic shift for stable isotope ratios of carbon, nitrogen, and sulfur. *Oikos* **111**(2): 416. DOI: <http://dx.doi.org/https://doi.org/10.1034/j.1600-0706.2003.12098.x>.
- McTigue, ND, Dunton, KH.** 2014. Trophodynamics and organic matter assimilation pathways in the north-east Chukchi Sea, Alaska. *Deep Res Part II* **102**: 84–96. Elsevier. DOI: <http://dx.doi.org/10.1016/j.dsr2.2013.07.016>.
- Michel, LN, Danis, B, Dubois, P, Eleaume, M, Fournier, J, Gallut, C, Jane, P, Lepoint, G.** 2019. Increased sea ice cover alters food web structure in East Antarctica. *Sci Rep* **9**(1). DOI: <http://dx.doi.org/10.1038/s41598-019-44605-5>.
- Michel, LN, David, B, Dubois, P, Lepoint, G, De Ridder, C.** 2016. Trophic plasticity of Antarctic echinoids under contrasted environmental conditions. *Polar Biol* **39**(5): 913–923. DOI: <http://dx.doi.org/10.1007/s00300-015-1873-y>.
- Müller, J, Wagner, A, Fahl, K, Stein, R, Prange, M, Lohmann, G.** 2011. Towards quantitative sea ice reconstructions in the northern North Atlantic: A combined biomarker and numerical modelling approach. *Earth Planet Sci Lett* **306**(3–4): 137–148. DOI: <http://dx.doi.org/10.1016/j.epsl.2011.04.011>.
- Navarro-Rodriguez, A, Belt, ST, Knies, J, Brown, TA.** 2013. Mapping recent sea ice conditions in the Barents Sea using the proxy biomarker IP₂₅: Implications for palaeo sea ice reconstructions. *Quat Sci Rev* **79**: 26–39. Elsevier Ltd. DOI: <http://dx.doi.org/10.1016/j.quascirev.2012.11.025>.
- Norkko, A, Thrush, SF, Cummings, VJ, Gibbs, MM, Andrew, NL, Norkko, J, Schwarz, AM.** 2007. Trophic structure of coastal Antarctic food webs associated with changes in sea ice and food supply. *Ecology* **88**(11): 2810–2820. DOI: <http://dx.doi.org/10.1890/06-1396.1>.
- North, CA, Lovvorn, JR, Kolts, JM, Brooks, ML, Cooper, LW, Grebmeier, JM.** 2014. Deposit-feeder diets in the Bering Sea: Potential effects of climatic loss of sea ice-related microalgal blooms. *Ecol Appl* **24**(6): 1525–1542. DOI: <http://dx.doi.org/10.1890/13-0486.1>.
- Nozais, C, Gosselin, M, Michel, C, Tita, G.** 2001. Abundance, biomass, composition and grazing impact of the sea-ice meiofauna in the North water, Northern Baffin Bay. *Mar Ecol Prog Ser* **217**: 235–250. DOI: <http://dx.doi.org/10.3354/meps217235>.
- Olivier, F, Gaillard, B, Thébault, J, Meziane, T, Tremblay, R, Dumont, D, Bélanger, S, Gosselin, M, Jolivet, A, Chauvaud, L, Martel, AL, Rysgaard, S, Olivier, A-H, Pettré, J, Mars, J, Gerber, S, Archambault, P.** 2020. Shells of the bivalve *Astarte moerchi* give new evidence of a strong pelagic-benthic coupling shift occurring since the late 1970s in the North Water polynya. *Phil Trans R Soc A*. **378**: 20190353. DOI: <http://dx.doi.org/10.1098/rsta.2019.0353>.
- Piepenburg, D.** 2005. Recent research on Arctic benthos: Common notions need to be revised. *Polar Biol* **28**(10): 733–755. DOI: <http://dx.doi.org/10.1007/s00300-005-0013-5>.
- Post, E.** 2017. Implications of earlier sea ice melt for phenological cascades in arctic marine food webs. *Food Webs* **13**: 60–66. Elsevier Inc. DOI: <http://dx.doi.org/10.1016/j.fooweb.2016.11.002>.
- R Core Team.** 2019. R: A language and environment for statistical computing. R Foundation for Statistical Computing, Vienna, Austria. Available at <https://www.R-project.org/>.
- Reid, WDK, Sweeting, CJ, Wigham, BD, McGill, RAR, Polunin, NVC.** 2016. Isotopic niche variability in macroconsumers of the East Scotia Ridge (Southern Ocean) hydrothermal vents: What more can we learn from an ellipse? *Mar Ecol Prog Ser* **542**: 13–24. DOI: <http://dx.doi.org/10.3354/meps11571>.
- Renaud, PE, Løkken, TS, Jørgensen, LL, Berge, J, Johnson, BJ.** 2015. Macroalgal detritus and food-web subsidies along an Arctic fjord depth-gradient. *Front Mar Sci* **2**: 1–15. DOI: <http://dx.doi.org/10.3389/fmars.2015.00031>.

- Renaud, PE, Tessmann, M, Evenset, A, Christensen, GN.** 2011. Benthic food-web structure of an arctic fjord (kongsfjorden, svalbard). *Mar Biol Res* **7**(1): 13–26. DOI: <http://dx.doi.org/10.1080/1745100103671597>.
- Riaux-Gobin, C, Klein, B.** 1993. Microphytobenthic biomass measurement using HPLC and conventional pigment analysis, in *Handbook in methods of aquatic microbial ecology*. Lewis Publishers: 369–376. DOI: <http://dx.doi.org/10.1201/9780203752746-43>.
- Ribeiro, S, Sejr, MK, Limoges, A, Heikkilä, M, Andersen, TJ, Tallberg, P, Weckström, K, Husum, K, Forwick, M, Dalsgaard, T, Massé, G, Seidenkrantz, M-S, Rysgaard, S.** 2017. Sea ice and primary production proxies in surface sediments from a High Arctic Greenland fjord: Spatial distribution and implications for palaeoenvironmental studies. *Ambio* **46**: 106–118. DOI: <http://dx.doi.org/10.1007/s13280-016-0894-2>.
- Rontani, JF, Belt, ST.** 2019. Photo- and autoxidation of unsaturated algal lipids in the marine environment: An overview of processes, their potential tracers, and limitations. *Org Geochem* **139**. DOI: <http://dx.doi.org/10.1016/j.orggeochem.2019.103941>.
- Rontani, JF, Belt, ST, Brown, TA, Amiraux, R, Gosselin, M, Vaultier, F, Mundy, CJ.** 2016. Monitoring abiotic degradation in sinking versus suspended Arctic sea ice algae during a spring ice melt using specific lipid oxidation tracers. *Org Geochem* **98**: 82–97. DOI: <http://dx.doi.org/10.1016/j.orggeochem.2016.05.016>.
- Rontani, JF, Belt, ST, Brown, TA, Vaultier, F, Mundy, CJ.** 2014. Sequential photo- and autoxidation of diatom lipids in Arctic sea ice. *Org Geochem* **77**: 59–71. DOI: <http://dx.doi.org/10.1016/j.orggeochem.2014.09.009>.
- Rontani, JF, Belt, ST, Vaultier, F, Brown, TA.** 2011. Visible light induced photo-oxidation of highly branched isoprenoid (HBI) alkenes: Significant dependence on the number and nature of double bonds. *Org Geochem* **42**(7): 812–822. DOI: <http://dx.doi.org/10.1016/j.orggeochem.2011.04.013>.
- Rossi, L, Sporta Caputi, S, Calizza, E, Careddu, G, Oliverio, M, Schiaparelli, S, Costantini, ML.** 2019. Antarctic food web architecture under varying dynamics of sea ice cover. *Sci Rep* **9**(1): 1–13. Springer US. DOI: <http://dx.doi.org/10.1038/s41598-019-48245-7>.
- Roy, V, Iken, K, Archambault, P.** 2014. Environmental drivers of the Canadian Arctic megabenthic communities. *PLoS One* **9**(7). DOI: <http://dx.doi.org/10.1371/journal.pone.0100900>.
- Roy, V, Iken, K, Gosselin, M, Tremblay, JÉ, Bélanger, S, Archambault, P.** 2015. Benthic faunal assimilation pathways and depth-related changes in food-web structure across the Canadian Arctic. *Deep Res Part I Oceanogr Res Pap* **102**: 55–71. Elsevier. DOI: <http://dx.doi.org/10.1016/j.dsr.2015.04.009>.
- Rybakova, E, Kremenetskaia, A, Vedenin, A, Boetius, A, Gebruk, A.** 2019. Deep-sea megabenthos communities of the Eurasian Central Arctic are influenced by ice-cover and sea-ice algal falls. *PLoS One* **14**(7): 1–27. DOI: <http://dx.doi.org/10.1371/journal.pone.0211009>.
- Smik, L, Cabedo-Sanz, P, Belt, ST.** 2016. Semi-quantitative estimates of paleo Arctic sea ice concentration based on source-specific highly branched isoprenoid alkenes: A further development of the PIP₂₅ index. *Org Geochem* **92**: 63–69. DOI: <http://dx.doi.org/10.1016/j.orggeochem.2015.12.007>.
- Stasko, AD, Bluhm, BA, Reist, JD, Swanson, H, Power, M.** 2018. Relationships between depth and $\delta^{15}\text{N}$ of Arctic benthos vary among regions and trophic functional groups. *Deep Res Part I* **135**: 56–64. Elsevier Ltd. DOI: <http://dx.doi.org/10.1016/j.dsr.2018.03.010>.
- Stern, HL, Heide-Jørgensen, MP.** 2003. Trends and variability of sea ice in Baffin Bay and Davis Strait, 1953–2001. *Polar Res* **22**(1): 11–18. DOI: <http://dx.doi.org/10.3402/polar.v22i1.6438>.
- Stoynova, V, Shanahan, TM, Huguen, KA, de Vernal, A.** 2013. Insights into Circum-Arctic sea ice variability from molecular geochemistry. *Quat Sci Rev* **79**: 63–73. DOI: <http://dx.doi.org/10.1016/j.quascirev.2012.10.006>.
- Tamelander, T, Reigstad, M, Hop, H, Ratkova, T.** 2009. Ice algal assemblages and vertical export of organic matter from sea ice in the Barents Sea and Nansen Basin (Arctic Ocean). *Polar Biol* **32**(9): 1261–1273. DOI: <http://dx.doi.org/10.1007/s00300-009-0622-5>.
- Tang, CCL, Ross, CK, Yao, T, Petrie, B, DeTracey, BM, Dunlap, E.** 2004. The circulation, water masses and sea-ice of Baffin Bay. *Prog Oceanogr* **63**(4): 183–228. DOI: <http://dx.doi.org/10.1016/j.pocean.2004.09.005>.
- Tedesco, L, Vichi, M, Scoccimarro, E.** 2019. Sea-ice algal phenology in a warmer Arctic. *Sci Adv* **5**(5). DOI: <http://dx.doi.org/10.1126/sciadv.aav4830>.
- Tremblay, JÉ, Hattori, H, Michel, C, Ringuette, M, Mei, ZP, Lovejoy, C, Fortier, L, Hobson, KA, Amiel, D, Cochran, K.** 2006. Trophic structure and pathways of biogenic carbon flow in the eastern North Water Polynya. *Prog Oceanogr* **71**(2–4): 402–425. DOI: <http://dx.doi.org/10.1016/j.pocean.2006.10.006>.
- Van Oevelen, D, Bergmann, M, Soetaert, K, Bauerfeind, E, Hasemann, C, Klages, M, Schewe, I, Soltwedel, T, Budaeva, NE.** 2011. Carbon flows in the benthic food web at the deep-sea observatory HAUSGARTEN (Fram Strait). *Deep Res Part I* **58**(11): 1069–1083. Elsevier. DOI: <http://dx.doi.org/10.1016/j.dsr.2011.08.002>.
- Vedenin, A, Gusky, M, Gebruk, A, Kremenetskaia, A, Rybakova, E, Boetius, A.** 2018. Spatial distribution of benthic macrofauna in the Central Arctic Ocean. *PLoS One* **13**(10). DOI: <http://dx.doi.org/10.1371/journal.pone.0200121>.
- Volkman, JK, Barrett, SM, Dunstan, GA.** 1994. C25 and C30 highly branched isoprenoid alkenes in laboratory cultures of two marine diatoms. *Org Geochem*

21(3–4): 407–414. DOI: [http://dx.doi.org/10.1016/0146-6380\(94\)90202-X](http://dx.doi.org/10.1016/0146-6380(94)90202-X).

Wang, SW, Budge, SM, Iken, K, Gradinger, RR, Springer, AM, Wooller, JM. 2015. Importance of sympagic production to Bering Sea zooplankton as revealed from fatty acid-carbon stable isotope analyses. *Mar Ecol Progress Ser* **518**: 31–50. DOI: <http://dx.doi.org/10.3354/meps11076>.

Wing, SR, McLeod, RJ, Leichter, JJ, Frew, RD, Lamare, MD. 2012. Sea ice microbial production

supports Ross Sea benthic communities: Influence of a small but stable subsidy. *Ecology* **93**(2): 314–323. DOI: <http://dx.doi.org/10.1890/11-0996.1>.

Xu, Y, Jaffé, R, Wachnicka, A, Gaiser, EE. 2006. Occurrence of C₂₅ highly branched isoprenoids (HBIs) in Florida Bay: Paleoenvironmental indicators of diatom-derived organic matter inputs. *Org Geochem* **37**(7): 847–859. DOI: <http://dx.doi.org/10.1016/j.orggeochem.2006.02.001>.

How to cite this article: Yunda-Guarin, G, Brown, TA, Michel, LN, Saint-Béat, B, Amiraux, R, Nozais, C, Archambault, P, 2020. Reliance of deep-sea benthic macrofauna on ice-derived organic matter highlighted by multiple trophic markers during spring in Baffin Bay, Canadian Arctic. *Elem Sci Anth.* 8: 1. DOI: <https://doi.org/10.1525/elementa.2020.047>.

Domain Editor-in-Chief: Jody W. Deming, University of Washington, Seattle, WA, USA

Associate Editor: Laurenz Thomsen, Jacobs University Bremen, Germany

Knowledge Domain: Ocean Science

Part of an Elementa Special Feature: Green Edge

Published: December 11, 2020 **Accepted:** October 31, 2020 **Submitted:** May 02, 2020

Copyright: © 2020 The Author(s). This is an open-access article distributed under the terms of the Creative Commons Attribution 4.0 International License (CC-BY 4.0), which permits unrestricted use, distribution, and reproduction in any medium, provided the original author and source are credited. See <http://creativecommons.org/licenses/by/4.0/>.

